**Pre-normative REsearch for Safe use of Liquid Hydrogen (PRESLHY)**

Project Deliverable

# Summary of experiment series E3.1 (Discharge) results Part A “High pressure gaseous hydrogen” and Part B “Low pressure liquid hydrogen”

| | |
|---|---|
| Deliverable Number: | 3.4 (D21) |
| Work Package: | 3 |
| Version: | 2.0 |
| Author(s), Institution(s): | A. Friedrich PS, A. Veser PS<br>T. Jordan, KIT |
| Submission Date: | 21 May 2021 |
| Due Date: | 30 November 2018 |
| Report Classification: | Confidential |

This project has received funding from the Fuel Cells and Hydrogen 2 Joint Undertaking under the European Union’s Horizon 2020 research and innovation programme under grant agreement No 779613.

| History | | |
|---|---|---|
| Nr. | Date | Changes/Author |
| 1.0 | 19.7.2019 | Original version by A. Friedrich, A. Veser and T. Jordan PS/KIT |
| 1.1 | 23.7.2019 | Sequential table of experiments in the Appendix A2;<br>Correction of electric field scale |
| 1.2 | 01.8.2019 | DOI https://doi.org/10.5445/IR/1000096833<br>as KITopen references |
| 2.0 | 21.05.2021 | Addition of Cryostat-experiments (Part B) by A. Friedrich (PS) |

| Approvals | | | |
|---|---|---|---|
| Version | Name | Organisation | Date |
| 1.1 - Draft | Simon Coldrick | HSL | 1 September 2018 |
| 1.x - Draft Part B | L. Bernard,<br>S. Jallais<br>A. Venetsanos | AL<br>AL<br>NCSRD | 30 April 2021 |

## Acknowledgements

This project has received funding from the Fuel Cells and Hydrogen 2 Joint Undertaking under the European Union's Horizon 2020 research and innovation programme under grant agreement No 779613.

## Disclaimer

The data management in the PRESLHY project follows the principle of data management, which shall make data Findable, Accessible, Interoperable and Re-usable (FAIR). The plan for FAIR data management as described in this document is based on the corresponding template for open research data management plan (DMP) of the European Research Council (ERC).

Despite the care that was taken while preparing this document the following disclaimer applies: The information in this document is provided as is and no guarantee or warranty is given that the information is fit for any particular purpose. The user thereof employs the information at his/her sole risk and liability.

The document reflects only the authors' views. The FCH JU and the European Union are not liable for any use that may be made of the information contained therein.

## Key Words

Cryogenic release, high pressure, discharge coefficient, jet dispersion, electrostatic field, far field observation

## Publishable Short Summary

In part A of WP3.1 of the PRESLHY project more than 200 hydrogen blow-down experiments were made with the DisCha-facility at KIT and about half of the experiments were made at cryogenic temperatures (approx. 80 K). During the experimental campaign the facility was continuously improved and extended, since several problems with the facility and instrumentation were encountered. However, the tests showed very good reproducibility.

Although the actual exploitation of the data is left for the further modelling work in the work packages WP3 and WP4, some interesting observations are: not a single test showed a spontaneous ignition, although the cold jets generated relative strong electrostatic fields. This static electricity seems to be generated by ice crystal which form on the release nozzle before the tests. The cold tests with large diameter and high pressure show strong temperature decay in the reservoir close to the boiling point of hydrogen and quite a huge fraction of “particles” entrained in the released jet were recorded. It is assumed that this is ice from ambient humidity and frozen on the nozzle before the actual test. However, there might be condensed hydrogen involved, as the acceleration of the gas through the nozzle might bring down the temperature below the boiling point. Only detailed multi-phase simulations accounting for non-equilibrium effects of the real gases’ behaviour might clarify this issue.

In part B of WP3.1 of the PRESLHY project 12 hydrogen blow-down experiments were performed with the Cryostat-facility on a free field-test site located a few kilometers to the north of KIT Campus North. About half of the experiments were made with liquid hydrogen at cryogenic temperatures (approx. 20 K). In the experimental campaign, the same release branch as in the related DisCha-experiments of Task 3.1A was used to facilitate comparison with the experiments of this series. For the same reason, five of the blow-down tests were made under ambient temperature conditions, since in part A also half of the matrix was performed under these conditions.

The tests showed very good reproducibility. Besides the discharge characteristics and the transient jet behavior also the electrostatic fields have been recorded to understand potential mechanisms for spontaneous ignition.

# Table of Contents

# Purpose of the Tests – Knowledge Gap Addressed

In the work package WP3.1 of the PRESLHY project the blow-down behavior of cryogenic hydrogen stored at elevated pressure is investigated by the project partners Karlsruhe Institute of Technology (KIT) and Pro-Science (PS).

In the first part A of the tests the DisCha facility is utilized to investigate releases of cryogenic hydrogen at temperatures of approximately 80 K and pressures up to 200 bar, and to compare this behavior with similar releases at ambient temperature. Therefore two experimental series, one at ambient temperature and the other at cryogenic temperature, the boiling temperature of liquid nitrogen ($LN_2$) were performed with DisCha facility. The facility was integrated in a larger experimental set-up, which was protected from too strong environmental influence with a tent. The set-up was installed on the free field behind the main hall of the hydrogen test site HyKa at KIT (see Figure **1**).

Figure 1: Location of DisCha-facility in a tent behind the main hall of the hydrogen test site HYKA at KIT.

Since no releases of liquid hydrogen ($LH_2$) were possible from the DisCha-facility, a Cryostat-facility was planned, fabricated and used to realize the release of $LH_2$ in part B of this task. In the Cryostat-experiments the blowdown behavior of liquid hydrogen ($LH_2$) stored at absolute pressures of up to 5 bar is investigated. In this work again two experimental series, one at ambient temperature as a reference and the main series at cryogenic temperature (in this case the temperature of $LH_2$, approx. 20 K) were performed. A photo of the Cryostat-facility on the free-field test site is shown in Figure **2**.

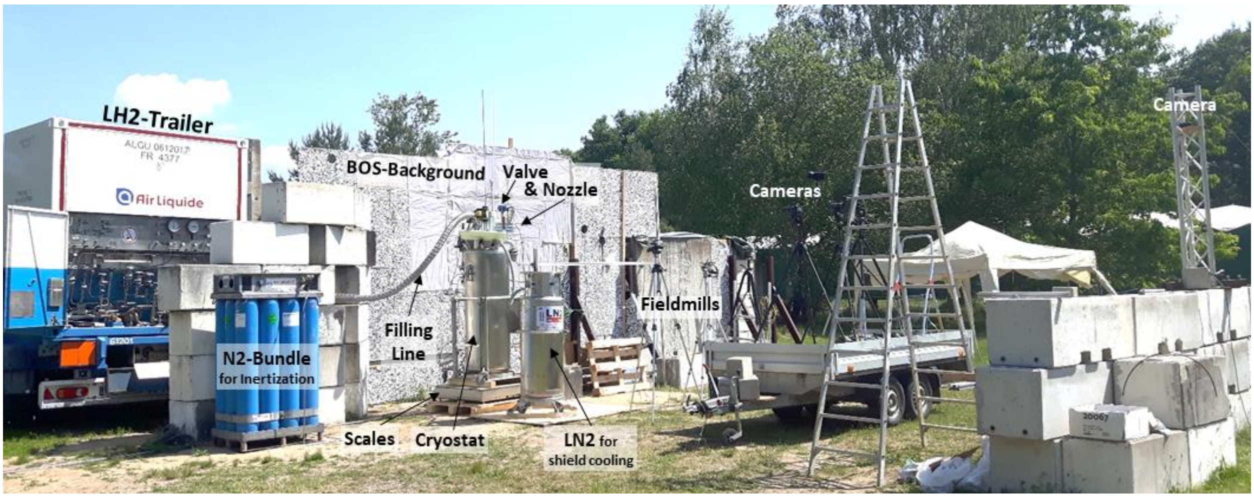


Figure 2: Photo of the setup of the Cryostat-experiments with $LH_2$ on the free-field test site north of KIT-Campus North.

The main purpose of WP3.1 was to provide validation or reference data for

- models defining or using a discharge coefficient,
- subsequent explosion tests, where the released gases will be ignited (see E5.2), and
- electrostatic field excitation and associated ignition potential of high-pressure hydrogen gas jets

at cryogenic temperatures.

# Part A: Experiments in the DisCha-Facility

## A-1 General Description of the DisCha-Facility

The DisCha facility mainly consists of a stainless-steel pressure vessel with an internal free volume of 2.815 dm³ and a weight of about 28 kg, which is fastened in an insulated box for the $LN_2$ pool cooling (Remark: the original plan to cool the DisCha facility with a $LH_2$ pool was discarded because of the high costs and the volatile boiling behavior expected for $LH_2$, and because the pressure vessel was only designed for $LN_2$ boiling temperature).

The cooling box with the vessel is mounted on a sledge and this sledge is mounted on a balance. The total weight of the experimental set-up, as measured by the balance is about 120 kg. Photographs of the facility and a sketch of the facility are shown in Figure A-**1** and Figure A-**2**.


Figure A-1: Photographs of the DisCha-pressure vessel (left) and the general set-up of the DisCha-facility (right).

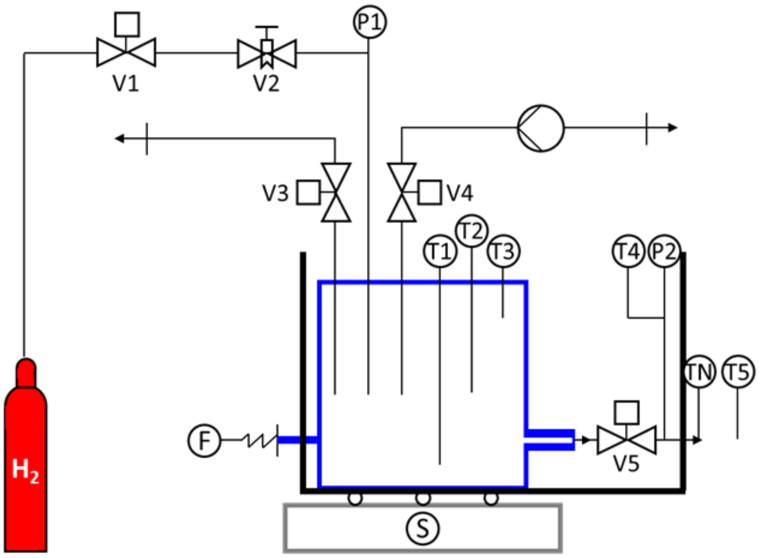


Figure A-2: Sketch of the DisCha-facility
(DisCha in blue color, cooling box in bold black color, balance in grey color).

Through the filling line and the valves V1 and V2 the test vessel can be filled with hydrogen up to pressures of 200 bar from a bundle of hydrogen bottles. The vessel is equipped with several ports for instrumentation on its top and a rod that points on a force sensor on its rear side. Opposite to the force sensor a tubular exhaust pipe is welded to the vessel, where release nozzles with different aperture sizes, nozzle diameters respectively, can be fastened.

The sledge provides an almost slip free movement of the setup for the measurement of the repulsive forces, that act on the vessel during the release experiments. The balance is used to measure the loss of weight caused by the effusing gas in the hydrogen release experiments.

Four nozzles with circular apertures of 0.5, 1, 2 and 4 mm were used in the experiments. The nozzles were mounted from outside the pool to the tube that connects them to the release valve (Figure A-**3**). Another connection, which is kept as short as possible, is mounted in between the release valve and the vessel exhaust

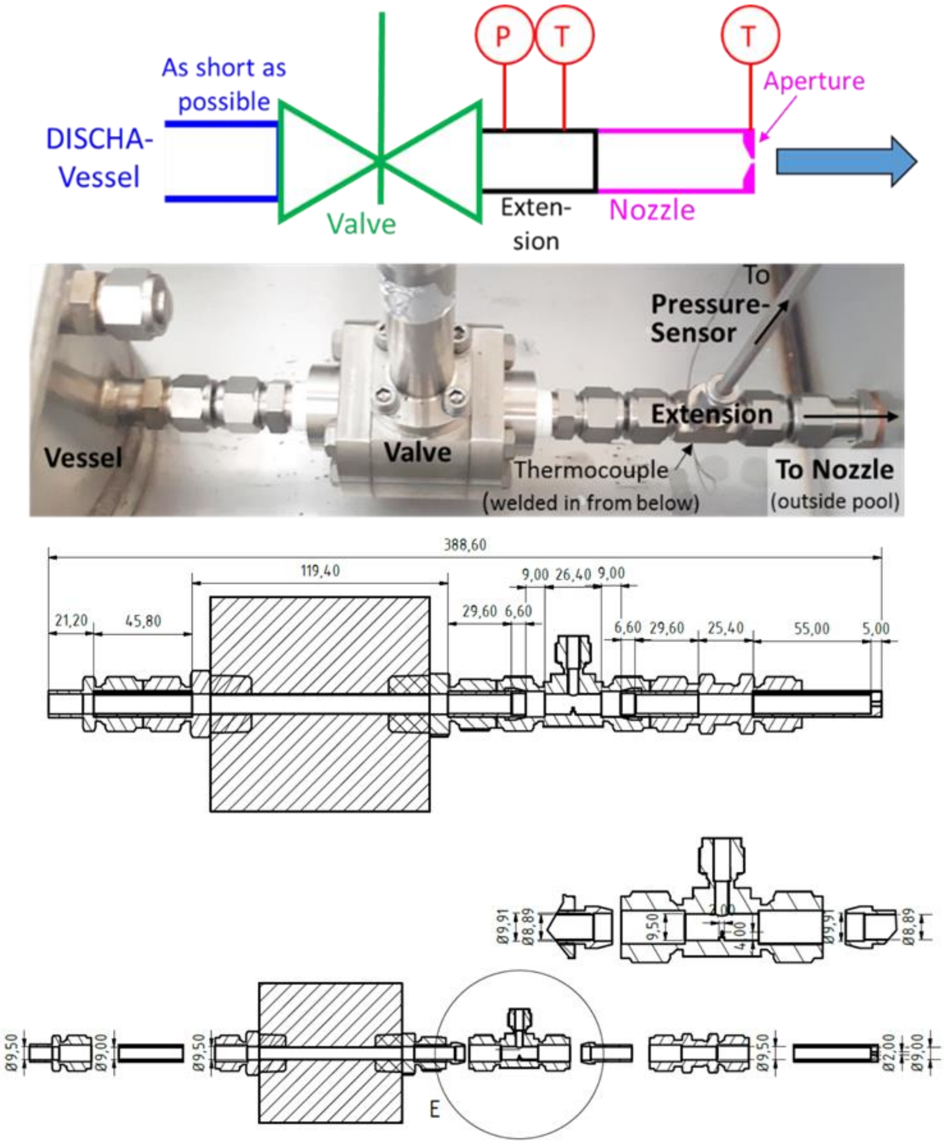


Figure A-3: Sketch, photo and technical drawing of the release pipework of the DisCha-facility with the 2 mm release nozzle (only diameter Ø 2 is changed for other nozzles).

In pre-tests, the opening-time of the valve was determined by filming (240 fps) the indicator disc at the top of the valve head in front of an optical clock that uses LED-bars in a binary logistic for indicating the time span that has elapsed after the trigger signal was issued. The disc is directly connected to the ball inside the ball valve and thus accurately indicates the degree of valve opening. Selected images of the movie and the estimation of the opening angle of the ball valve are shown in Figure A-**4**.

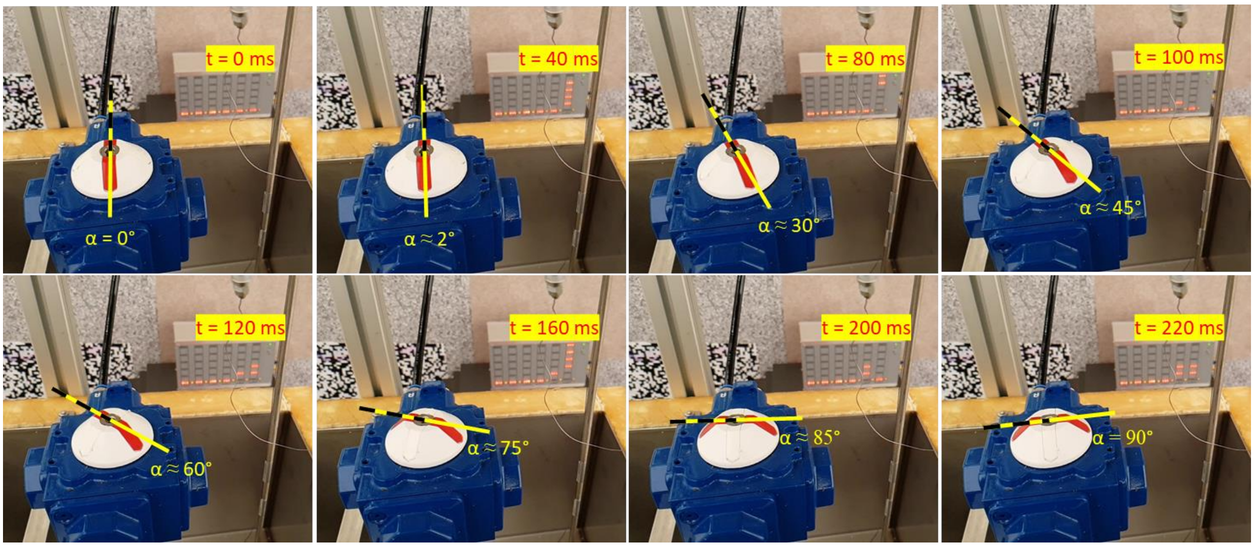


Figure A-4: Images from the movie taken to determine the opening time of the valve. Below the yellow time-labels in the images is the optical clock (Lowest LED-bar in columns indicates 0, lighted bars above on far-right side indicate 10 ms to 50 ms. LEDs are then quenched from 60 to 100 ms. For 100 ms first bar above zero in next column is illuminated).

From the pre-tests a valve-delay time of 40 ms is determined, after which the valve shows its first movement. During the following 180 ms the valve then opens completely.

## A-2 Instrumentation of the DisCha-Facility

### Sensors and Methods used in the DisCha-Facility

Apart from the force sensor (Althen, Type ALF318CPR0K0, 0 - 2 kN) and the balance (Mettler-Toledo, PBA430x, 0 - 150 kg, F and S in Figure A-**2**), the test vessel and the release nozzle are instrumented with two pressure sensors and eight thermocouples. Outside the release nozzle further five thermocouples and a set of five $H_2$-concentration measurement devices are installed. Additionally, two field mills for measuring static electric field strength and three cameras (2 photo cameras and 1 video camera) are used to monitor the releases using the BOS-technique for the visualization of density gradients.

<u>Pressure sensors:</u> One static pressure sensor (P1 in Figure A-**2**) in the filling line is used to control the initial pressure inside the vessel during the filling procedure, while the second one measures the pressure changes in the release line. Since the second sensor is connected to the tube in between release valve and nozzle, the first increase in this signal corresponds to the actual start of the release. After the initial pressure built-up in the release line both pressure sensors capture the pressure decrease inside the vessel during the experiment.

Thermocouples (TCs): Three sets of NiCr/Ni-thermocouples (Type K) are used in the DisCha facility. Two sets (three TCs each) are installed inside the vessel to record the gas temperature during the experiment in different heights. The two sets are used to check the accuracy and the rise time of the three standard TCs (T1 to T3, diameter 0.36 mm, sensitive tip covered by thin stainless steel shell) with a second set of three very thin open TCs (T1o to T3o, diameter 0.25 mm, stainless steel shell of sensitive tip removed) that are no longer available at the workshop at KIT. Both sets are installed in comparable positions inside the vessel. In the release line two further standard TCs are positioned: T4 is welded into the line to measure the temperature inside it, while TN is mounted from the outside in a hole in the material of the stainless steel nozzle aperture with no direct contact to the flowing gas. In total five standard TCs are distributed outside the release nozzle. Three of these (T5 to T7) are located in distances of 250 mm, 750 mm and 1750 mm from the nozzle on its centerline, while T8 and T9 are positioned in distances of 250 mm and 500 mm slightly to the right and to the left of the nozzle centerline (see Figure A-**5**).

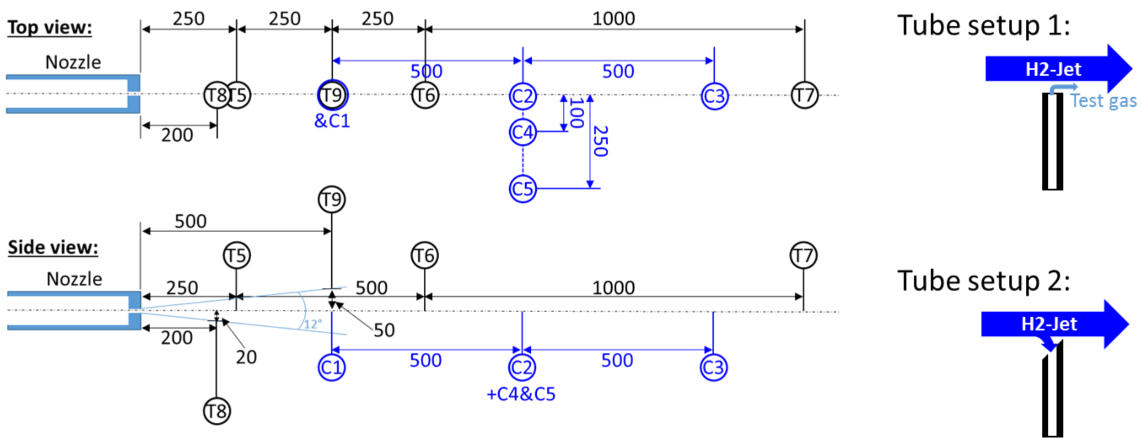


Figure A-5: Sketches of the ex-vessel instrumentation of the DisCha-facility and configurations of the plastic tubes for the $H_2$-concentration measurements.

Concentration measurements: Five Messkonzept $H_2$-sensors are utilized to determine the hydrogen concentration in different positions in the free hydrogen jet release. Three of these positions are on the jet axis, while the remaining two positions are in different horizontal distances to the jet centerline (see Figure A-**5**). Since these sensors are quite large and require a constant gas flow they were not mounted physically to the positions shown in **Fehler! Verweisquelle konnte nicht gefunden werden.**, but were connected to these positions via thin plastic tubes of 2.55 m length. One small pump is used to supply all sensors with the same volume flow of test atmosphere during the measurements. In pre-experiments the delay time due to this setup was determined by exposing the open tip of the plastic tube with pure or diluted hydrogen (20% $H_2$, forming gas) from a balloon (without forcing an additional flow of the test gas in the tube). A similar delay time of 2 s was found for all five sensors in this setup from the opening of the hydrogen balloon to the first increase in the signals of the hydrogen sensors.

In the first test series the open tip of the plastic tube was pointing straight upwards, with the planar cross section of the tube as horizontal plane in the jet centerline (tube setup 1 in Figure A-**5**). While evaluating the test records after the first series it was found that this setup causes irregularities in the arrival times, since the first sensor besides the centerline C4 detected hydrogen prior to C1, which is located much closer to the nozzle. The reason for this unrealistic behavior is most likely the fast flow passing the tip of the plastic tube, causing a suction effect in the tube which leads to an additional delay time for the transport of the test gas to the sensor (tube setup 1 in Figure A-**5**).

To avoid this effect all experiments were repeated once with a tilted cut of the plastic tube, with the open side of the cut pointing towards the nozzle (tube setup 2 in Figure A-**5**). But since the sensor of position C5 never detected significant amounts of $H_2$ in all experiments, it was decided to use this channel for reference measurements in position C1 with the old tube configuration (column H: C1-). Due to this change in the setup the hydrogen arrival times became more realistic, but in some cases with very high initial pressures hydrogen was detected already before the release valve was even opened. In this case the fast jet pushed the gas inside the tube which led to shorter delay-times than the 2 s determined for cases without any additional flow.

<u>Field mills:</u> Two field mills (model Kleinwächter EFM 113B) were positioned in the height of the nozzle in distances of 0.5 and 1.5 m from it and with horizontal distances of 0.9 m from the jet axis (see Figure A-**6**).

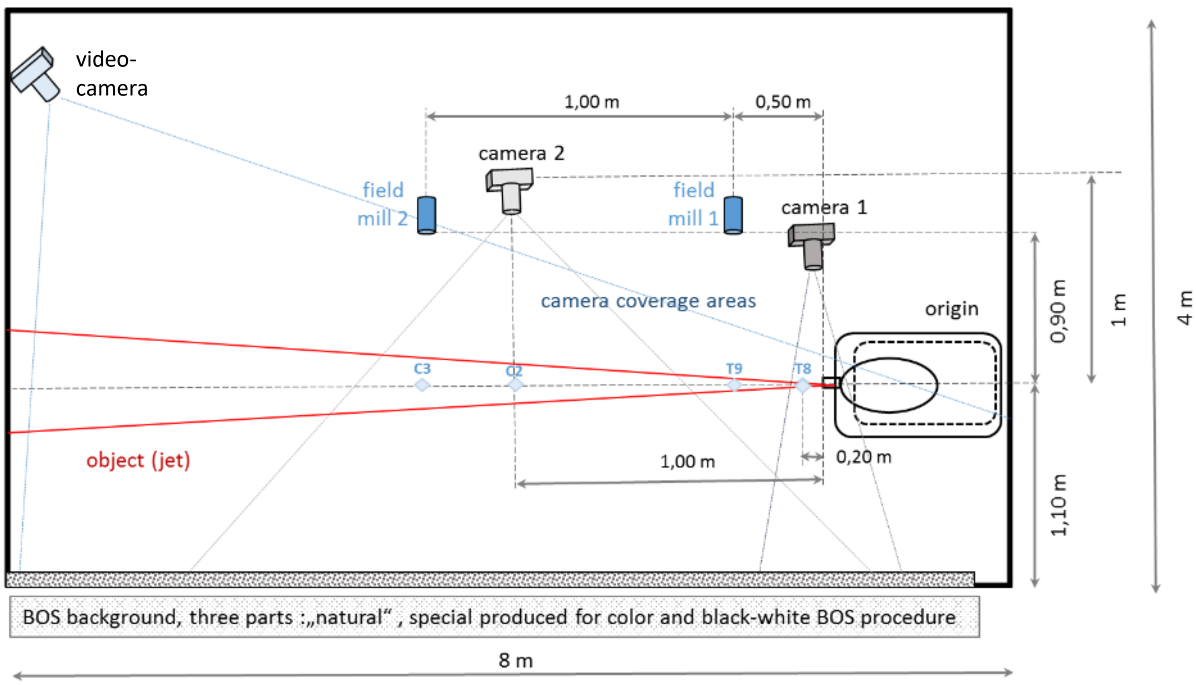


Figure A-6: Sketch of the positions of the field mills and the cameras in the DisCha-facility (top view).

<u>Cameras:</u> The two photo-cameras were positioned at 5 cm (Camera 1) and 1 m (Camera 2) in jet downstream direction, on the same height as the center of the release nozzle and with a distance of 0.9 m (Camera 1) and 1.1 m (Camera 2) to the horizontal center line, the nominal jet center line (see Figure A-6 and Figure A-7). The specifications of the two cameras are as follows:

<u>Camera 1</u>
CANON EOS5D Mark I

- lens type telephoto
- resolution 4368 x 2912 pixels
- distance from camera to horizontal release axis equals to 0.9 m
- the size of the observation area in the central jet plane is about 0.33 x 0.22 m

<u>Camera 2</u>
CANON EOS5D Mark II

- lens type wide angle
- resolution 5616 x 3744 pixels
- distance from camera to horizontal release axis equals 1.1 m
- the size of the observation area in the central jet plane is about 1.25 x 0.83 m (Version 1) or about 1 x 0.67 m (Version 2)

The photos were synchronized with the release time by utilizing a high-speed optical clock (see Figure A-**8**), which shows changing LED-signals to indicate the time that has passed after was initiated.

The video-camera was positioned below the roof of the tent in a distance of several meters downstream the nozzle pointing towards the release. To the right of the jet, opposite to the two photo-cameras, different background patterns were glued to wooden walls to test the BOS optical method for the visualization of the cold hydrogen jet releases. In the part close to the nozzle a fine random black and white box-pattern was used, while in farther distances "natural" backgrounds (branches and shrubs) were tested.

Figure A-7: Position of cameras and BOS background patterns on floor and back wall.

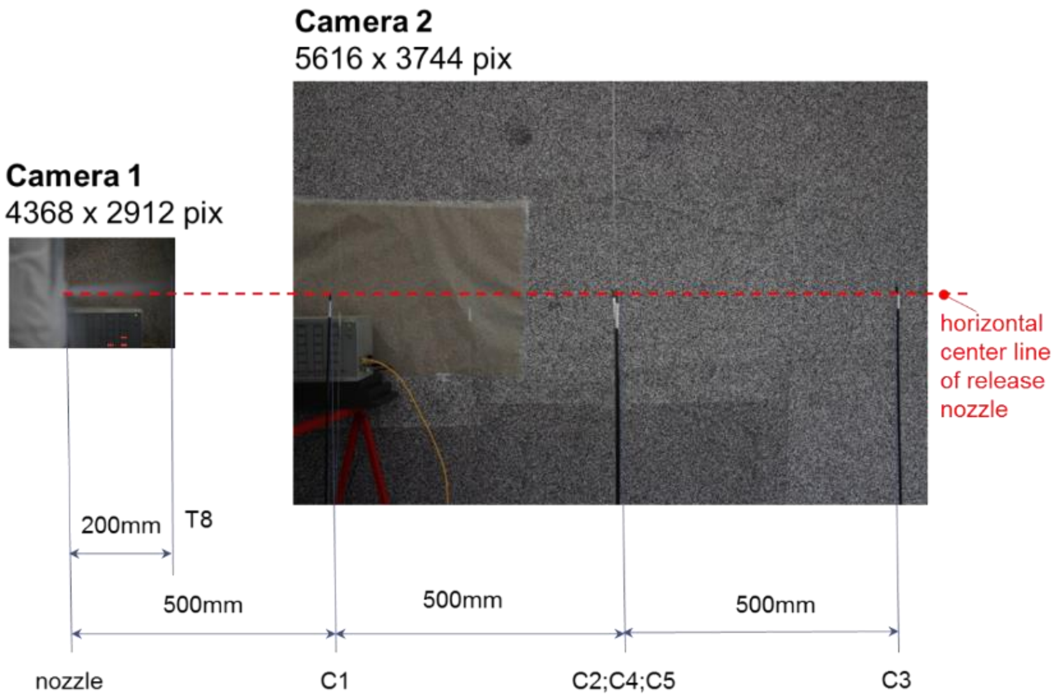


Figure A-8: View fields of the cameras related to special elements of the experimental set-up, Version 1 (nozzle on the left end of the horizontal center line; thermocouples T8, concentration sensors C1, C2, C4 and C5); optical clock visible in both photographs

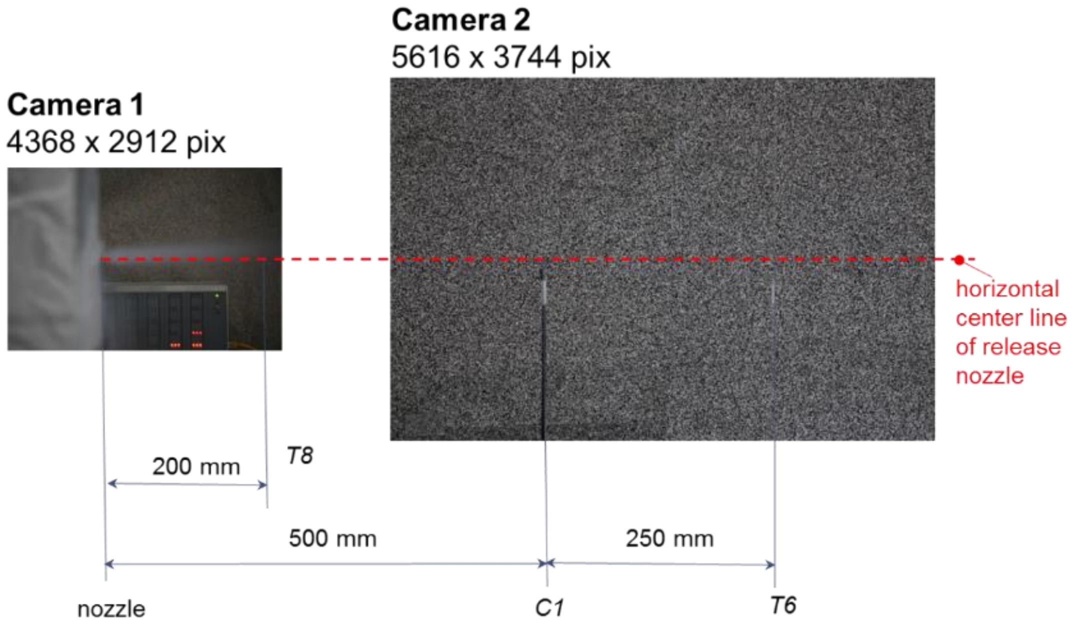


Figure A-9: View fields of the cameras related to special elements of the experimental set-up, Version 2 (nozzle on the left end of the horizontal center line; thermocouples T8 and T6, concentration sensor C1), optical clock on visible for Camera 1.

### Estimate of Measurement Errors

The accuracy of the sensors used in the experiments is given in Table A-**1** below. The values were taken from the respective manuals for ambient temperature conditions. For cryogenic temperatures no data is available.

Table A-1: Accuracy of the sensors used in the DisCha experiments.

| Sensor | Manufacturer | Type (Range) | Non-linearity @ 290 K |
|---|---|---|---|
| Force | Althen | ALF318CPR0K0 (2 kN) | ± 0,1 % FS |
| Scales | Mettler-Toledo | PBA430x (150 kg) | 0.006% FS |
| Pressure | WIKA | S-20 (250 bar) | < 0,125% FS |
| Field mill | Kleinwächter | EFM 1138 (5 kV/m) | < 5% FS |
| $H_2$-Sensor | Messkonzept | FTC300 (100% $H_2$) | < 1% FS |
| Temperature | KIT-Workshop | Type K, d = 0.36 mm | 1.66 °C |

In the experiments only the thermocouples are exposed to cryogenic temperatures and so their deviation from the temperature of $LN_2$ (77 K) was measured in a separate test. In this test all closed thermocouples (T1 – T9 and $T_{Nozzle}$, except T4, which is not accessible since it is welded into the extension tube) showed similar values of approx. 84 K, which corresponds to a difference of +7 K. The three open thermocouples T1o, T2o and T3o, used additionally inside the test vessel, were also tested in the same way, but showed quite large deviations with values of approximately 105 K for the temperature of liquid nitrogen. The reason for this behavior might be a combination of their age (about 10 years) and the open tip that might already show some degeneration. These sensors could not be replaced by new ones, since this type is no longer available at the KIT workshop. Because of their lower thermal capacities, their signal might be used to determine characteristic changes in time rather than to read accurate, absolute temperature values.

## A-3 Test Matrix of the DisCha-Experiments

The test matrix for the blow-down experiments was constructed by varying the release nozzle diameter (4 diameters: 0.5, 1, 2 and 4 mm) and the initial hydrogen storage pressure (7 nominal pressure values: 5, 10, 20, 50, 100, 150 and 200 bar) for two hydrogen storage temperature levels (2 nominal storage temperatures: 80 and 300 K). Typically, at least three repetitions of one pressure/nozzle diameter combination were conducted. In many cases the test has been repeated more than three times, for 200 bar and 2 mm even seven tests were done to provide an estimate for the stability, reproducibility respectively, of the measurement system in general.

The whole test campaign with more than 224 tests lasted almost 4 months (middle of February to end of June 2019) with several interruptions for improving the measurement set-up, setting up the pre-cooling or because of delays in $LN_2$ supply. Several pre-tests have been excluded from this report. Also those tests have been excluded, which were used to validate the modified concentration measurement, which is explained in Chapter A-3 above.

The test itself and the respective result files are labeled with the date and time (“date”_”time”), at which the test was initiated:

2019**MMDD_hhmmss**(**.ext**)

with **MM** for month, **DD** for day, **hh** for hour, **mm** for minute, **ss** for second of the formal start of the experiment; **ext** is either empty for just labelling the experiment, “xlsx” for the Excel files containing the dataset or “zip” for the set of photographs, pictures respectively, taken from this experiment.

The labeling of the zip-files containing several of those data or picture files for identical nozzle diameter and temperature is explained below.

All tests are listed in sequential order together with the information about effective initial temperature and pressure and about nozzle diameter in Appendix A2. This helps in finding the parameters associated with each test simply via its “date”_”time” name. The reference tests done first with hydrogen at ambient temperature are summarized in the test matrix shown in Table A-2. The test matrix for the cold experiments done with $LN_2$ cooling - the actual cryo-release tests - is shown in Table A-3.

In both tables the experiments, for which the datasets are published as via https://doi.org/10.5445/IR/1000096833 on KITopen [1], are highlighted with black bold font. The labels of those experiments, for which photographs are published also via KITopen, have a grey background color.

The cold tests 20190528_104204 (i.e. the test, which started 28th of May 2019 at 10:42 am) and for photography 20190503_140045 are used as representative examples in the further text.

Table A-2: Test matrix of DisCha experiments at ambient temperature
($n_{total}$= 126, experiment label 2019MMDD_hhmmss for start date and time).

| Pressure [bar] | Nozzle-Diameter [mm] 0.5 | 1 | 2 | 4 |
|---|---|---|---|---|
| 5 | ~~20190218_152803~~<br>~~20190218_153211~~<br>20190312_140742<br>**20190523_155208** | ~~20190218_145937~~<br>~~20190218_150203~~<br>20190312_141636<br>**20190523_151618** | ~~20190218_143922~~<br>~~20190218_144147~~<br>20190312_142444<br>**20190523_144219** | ~~20190218_135240~~<br>~~20190218_135848~~<br>~~20190221_105323~~<br>20190312_143216<br>**20190523_141327** |
| 10 | ~~20190218_153516~~<br>~~20190218_154048~~<br>20190312_141024<br>20190523_154849 | ~~20190218_150528~~<br>~~20190218_150851~~<br>20190312_141909<br>20190523_151411 | ~~20190218_144358~~<br>~~20190218_144713~~<br>20190312_142706<br>**20190523_144022** | ~~20190218_140223~~<br>~~20190218_140530~~<br>~~20190221_110229~~<br>20190312_143846<br>**20190523_141008** |
| 20 | ~~20190218_154318~~<br>~~20190218_154510~~<br>**20190523_154414** | ~~20190218_151140~~<br>~~20190218_151621~~<br>**20190523_151013** | ~~20190218_145002~~<br>~~20190218_145411~~<br>**20190523_143801** | ~~20190218_140858~~<br>~~20190218_141305~~<br>**20190523_140705** |
| 50 | 20190307_143703<br>20190326_152315<br>20190523_153958 | 20190307_141026<br>20190326_144506<br>20190326_144755<br>20190523_150640 | 20190307_111816<br>20190307_113513<br>20190326_140441<br>20190326_140752<br>**20190523_143501** | ~~20190221_110511~~<br>~~20190221_111257~~<br>20190307_133159<br>20190523_140344<br>**20190624_145615** |
| 100 | 20190307_144122<br>20190326_151458<br>20190326_151931<br>**20190523_153415** | 20190307_141324<br>20190326_143750<br>20190326_144109<br>**20190523_150133** | 20190307_113815<br>20190326_135707<br>20190326_140034<br>20190523_143020<br>**20190624_152500** | ~~20190221_140324~~<br>~~20190221_140517~~<br>~~20190221_141846~~<br>20190307_133454<br>20190322_104748<br>20190523_115747<br>**20190624_145052** |
| 150 | 20190307_144458<br>20190326_150440<br>20190326_150854<br>20190523_152829 | 20190307_142436<br>20190326_142958<br>20190326_143412<br>20190523_145700 | ~~20190221_150608~~<br>~~20190221_150950~~<br>20190307_114105<br>20190326_135313<br>20190523_142651<br>**20190624_151944** | ~~20190221_142431~~<br>~~20190221_142819~~<br>20190307_135327<br>20190322_103008<br>20190523_113338<br>**20190624_144205** |
| 200 | 20190307_144904<br>20190326_145458<br>20190326_150007<br>**20190523_152309** | 20190307_141656<br>20190326_141916<br>20190326_142523<br>**20190523_144939** | ~~20190221_143934~~<br>~~20190221_144801~~<br>~~20190221_145609~~<br>~~20190221_150110~~<br>20190307_114908<br>20190326_134758<br>20190523_142245<br>**20190624_151045** | ~~20190221_143129~~<br>~~20190221_142424~~<br>20190307_134340<br>20190307_140303<br>20190322_100645<br>20190523_113015<br>**20190624_143040** |

Published Excel **datasets** for instance in:
PRE3P1A_KIT_**D05_300K**_DATA.zip
corresponding photographs in
PRE3P1A_KIT_**D05_300K**_PICS.zip

Legend:

~~Not processed, no sync.~~
Not processed, sync. difficult
~~Processed, no sync.~~
Processed and synchronized
~~Published Photo~~graphs
**Published Datasets**

Table A-3: Test matrix of DisCha experiments at $LN_2$-temperature
($n_{total}$= 98, experiment label 2019MMDD_hhmmss for start date and time).

| | | Nozzle-Diameter [mm] | | | |
|---|---|---|---|---|---|
| | | 0.5 | 1 | 2 | 4 |
| Pressure [bar] | 5 | 20190509_143959<br>20190509_144955<br>20190604_151150<br>**20190604_153521** | 20190507_155308<br>20190507_160047<br>**20190531_120333** | 20190430_150817<br>20190430_151117<br>**20190531_103828** | 20190503_112024<br>20190503_112408<br>**20190528_111918** |
| | 10 | 20190509_142254<br>20190509_143252<br>20190604_150515<br>20190604_152905 | 20190507_153753<br>20190507_154609<br>20190531_115603 | 20190430_144909<br>20190430_150600<br>**20190531_103408** | 20190503_110955<br>20190503_111525<br>**20190528_111240** |
| | 20 | 20190509_111408<br>20190509_112201<br>20190604_145638<br>**20190604_152254** | 20190507_152321<br>20190507_153041<br>**20190531_114903** | 20190430_143105<br>20190430_144308<br>**20190531_102810** | 20190503_110259<br>20190503_121635<br>**20190528_110441** |
| | 50 | 20190509_135757<br>20190509_141151<br>20190604_144425 | 20190507_150252<br>20190507_151256<br>20190531_113940 | 20190430_141445<br>20190430_142516<br>**20190531_101948** | 20190503_115334<br>20190503_120719<br>**20190528_105437** |
| | 100 | 20190509_132731<br>20190509_134535<br>**20190604_142752** | 20190507_143257<br>20190507_144631<br>**20190531_112944** | 20190423_120305<br>20190430_111836<br>20190430_114028<br>**20190531_101249** | 20190503_104121<br>20190503_105250<br>20190528_112837<br>**20190528_143608** |
| | 150 | 20190509_104138<br>20190509_105344<br>20190604_140657 | 20190507_135605<br>20190507_141457<br>20190531_111808 | 20190423_121441<br>20190430_135153<br>20190430_140732<br>**20190531_100257** | 20190503_100144<br>20190503_102600<br>**20190528_142048** |
| | 200 | 20190509_100955<br>20190509_102557<br>**20190604_134543** | **20190531_110440** | 20190430_102456<br>20190430_110643<br>**20190531_094951** | 20190503_134536<br>20190503_140045<br>**20190528_104204** |

Published Excel **datasets** for instance in:
PRE3P1A_KIT_**D1_80K**_DATA.zip
corresponding photographs in
PRE3P1A_KIT_**D1_80K**_PICS.zip

Legend:

Not processed, sync. difficult
Processed, wrong format, sync. difficult
~~Processed, no sync.~~
Processed and synchronized
Published Photographs
**Published Datasets**
**used for further explanations**

## A-4 Structure of DisCha Experimental Result Data explained with Cold Case 20190528_104204

All experimental data of the unignited DisCha tests highlighted (in black bold font) in Table A-2 and Table A-3 are published as zipped Microsoft Excel-files via the PRESLHY repository on KITopen[1] in packages with identical nozzle diameter, separately for the ambient (referring to Table A-2 and labeled "300K") and cryogenic (referring to Table A-3 and labeled "80K") hydrogen temperatures, what corresponds to the respective columns in the above tables. Photographs of the camera 1 and camera 2 have been packed in zip-files per experiment, and then - similarly as for the Excel datasets - packed in larger zip-files for same diameter and temperature.

So, the naming convention of the corresponding zip-files follows in principle the one provided in the PRESLHY Data Management Plan[2] and reads as follows:

PRE3P1A_KIT_D**mm_tt**K_**extn**.zip

with **mm** indicating the nozzle diameter ("05","1","2" or "4"), **tt** the nominal start temperature ("80" for $LN_2$ boiling or "300" for ambient) and **extn** the type of data contained ("DATA" for Excel sheets containing all numerical and some predefined graphs, "PICS" for the photographs taken with camera 1 and 2). Two examples for the large zip-files are shown Table A-2 and Table A-3. For the preparation of the zip-files the free software 7-Zip[3] (64 bit version 19.0) has been used.

### Structure of the Datasets

The result data, the datasets respectively, are stored in Microsoft Excel files with the *.xlsx extension. Each Excel file consists of 4 worksheets, corresponding to the 4 different data acquisition systems/routines applied in the experiments. The Excel-files are named with same "date_time" convention as the experiments with the format "2019MMDD_hhmmss.xlsx". Compared to the raw data gained from the measurement system, only an additional top line and the column A were added to provide English column names and an additional, synchronized time, which corresponds to the time after the release valve was opened.

Due to improvements and additions the test set-up became more and more complex with increasing test number. So, the structure of the data is explained using one of the last experiments as an example: 20190528_104204, an experiment with 80 K, 4 mm nozzle and initial nominal pressure of 200 bar. The detailed results of this experiment are additionally provided in the Appendix A1 in form of result diagrams, as they are prepared and included in the Excel files also for all other experiments. If specific columns are missing in some Excel file, typically for experiments done earlier, this solely indicates that the corresponding sensor was not yet implemented at the time the data was recorded.

---

[1] https://doi.org/10.5445/IR/1000096833

[2] https://www.hysafe.info/wp-content/uploads/sites/3/2018/10/PRESLHY_D1_3_DataManagementPlanV1_4.pdf

[3] https://www.7-zip.org/

The first sheet of the Excel-file, named “20190528_104204-**Press**”, contains the data of the fast pressure measurements and, in the later stage, a column for the signal of the release valve (see Figure A-**10**). In the cells A2 and F2 the nozzle diameter and the initial pressure (as mean value of the last 5 s before the release valve was opened) of the experiment are given. In the upper row of graphs to the right of the data the beginning of the experiment is shown using the original time (column B) of the record, which was started some time before the release valve was opened. In the blue box above these graphs the times of the first changes in the records of all four data sheets of the Excel-file are summarized. So in line 3 the beginning times of the three sensor records of the current sheet are given, with the background of the cell corresponding to the color of the line in the graphs. In all cases the relay's signal increases first, followed by the pressure sensor in the release line (Pnoz) and the sensor in the test vessel (Pves). The grey highlighted cell O3 gives the delay time between relay and Pnoz, which corresponds to the valve delay time. This delay time is not a constant value but changes slightly with changing initial pressure and more pronounced with decreasing temperature.

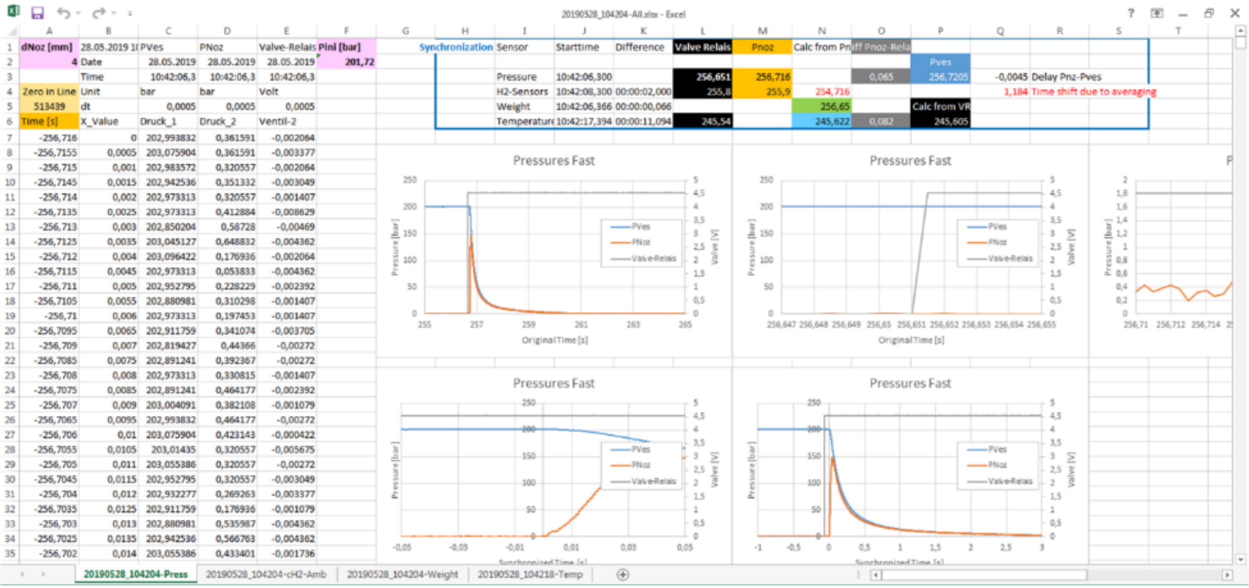


Figure A-10: Example for the structure of the first data sheet with the fast pressure measurements in the Excel-file of experiment 20190528_104204 at $LN_2$-temperature (4 mm nozzle, 200 bar).

For the synchronization the time of the first significant pressure increase in the release line (Pnoz) was used as t = 0, since this sensor is the one that detects the effusing hydrogen first (see Figure A-**11**). So the time of this first pressure increase (cell M3) was subtracted from the value of column B to yield the new synchronized time in column A. The initial phase of the experiment using this synchronized time is shown in the lower row of graphs. Due to the extremely high frequency of the pressure measurements (2 kHz) and the long test duration it is not possible to draw a graph in Excel showing the complete signal histories for all experiments.

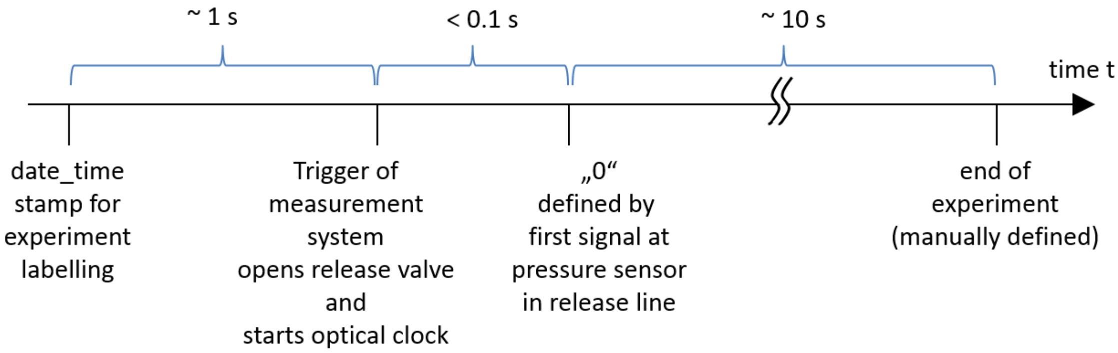


Figure A-11: Characteristic times of a DisCha blow-down experiment.

The second sheet of the Excel-file is named “20190528_104204-**cH2-Amb**” (Figure A-**12**) and is recorded with a much lower frequency (10 Hz), since most of the sensors recorded are not able to provide faster measurements. For synchronization the pressure sensors and the valve relay are recorded again. Further signals of the sheet are: $H_2$-concentrations, force-sensor, ambient humidity and temperature, as well as the signals of the two field mills used in the late test series. The last column of the sheet contains a second new time scale, in which the time delay of the $H_2$-sensors due to the transport time of the sample from the measuring position to the sensor itself is considered (delay time 2 s, see above in section concentration measurements of chapter A-2 Instrumentation of the DisCha-Facility).

In the uppermost two graphs the synchronization is demonstrated by showing two graphs with the pressure signals over original and synchronized time. Then the records of the $H_2$-sensors are plotted with their corrected time (including 2 s time delay), followed by graphs of the other sensor signals of this worksheet. In the blue box above the graphs again the times of the first changes in the records of the pressure sensors of all data sheets are summarized. The corresponding times of the current sheet are listed in line 4.

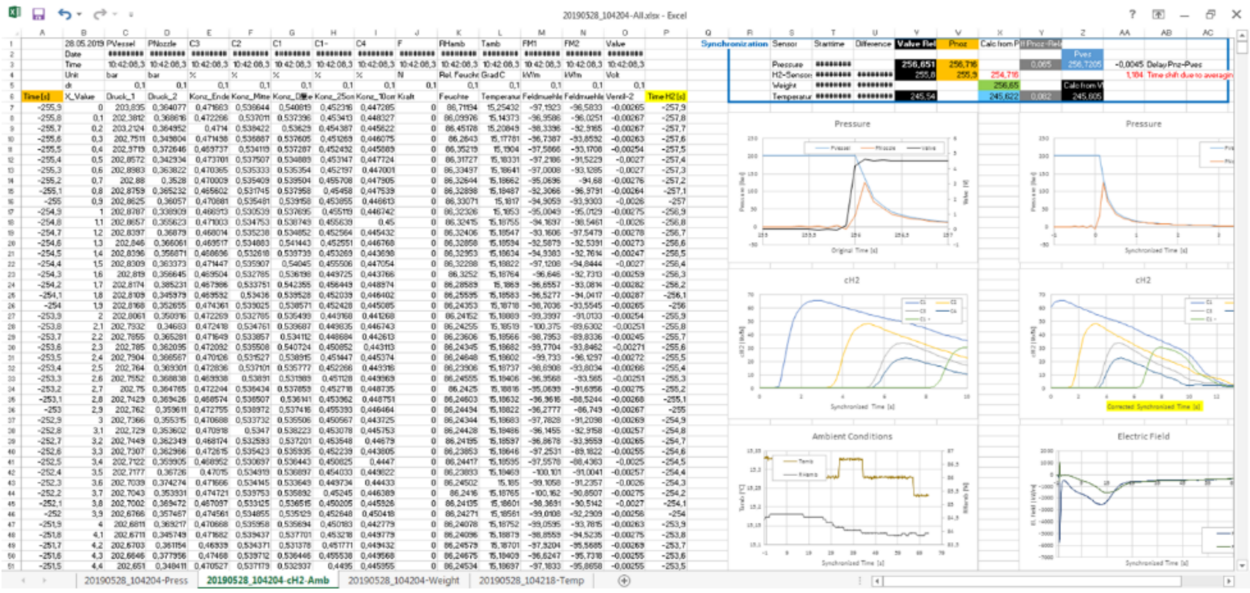

Figure A-12: Example for the structure of the second data sheet with $H_2$-concentration and force measurements, the ambient conditions and the field-mill records in the Excel-file of experiment 20190528_104204 at $LN_2$-temperature (4 mm nozzle, 200 bar).

The third sheet has the name "20190528_104204-**Weight**" and contains only the data recorded by the scales with its maximum frequency of 2 Hz (see Figure A-**13**). Due to software problems this sensor had to be recorded separately, and thus no other signal for the synchronization is available. In this case the opening time of the valve is calculated using the generation time of the data-file, which is given in line 3 in all column headers. The difference between the fast pressure records (first sheet in Excel-file) and the scales data is calculated in cell K5 and the result is used to generate the synchronized time in column A. Signal histories of the scales record with the original and the synchronized time are shown in the two graphs of the sheet.

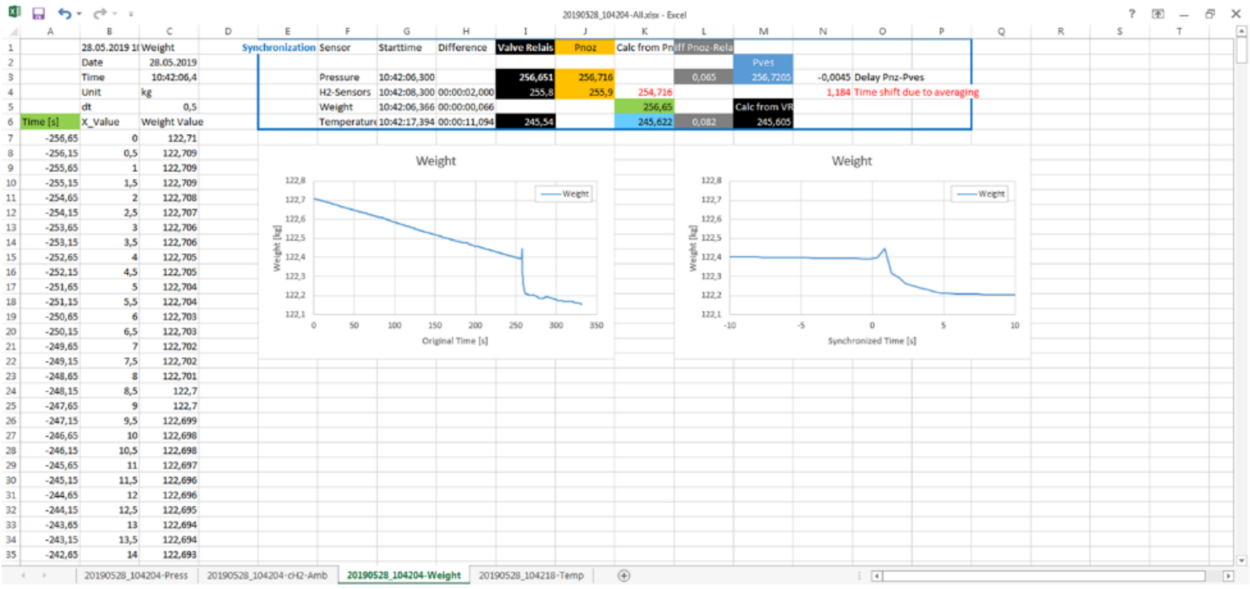

Figure A-13: Example for the structure of the third data sheet with balance-records in the Excel-file of experiment 20190528_104204 at $LN_2$-temperature (4 mm nozzle, 200 bar).

The last sheet of the Excel-file has the name "20190528_104218-**Temp**" and contains the temperature measurements in- and outside the test vessel with the maximum frequency of 100 Hz (see Figure A-**14**). Additionally, the signal of the valve relay is recorded for synchronization. Since a different routine was necessary to record the temperatures a record of Pnoz together with the thermocouples was not possible (and for the same reason the time in the name of this sheet is slightly different from the time in the names of the other sheets). So a synchronization can be either made by a comparison of the generation times of the data-files (line 3) or a synchronization via the relay time, which was also recorded with the fast pressure sensors (see first sheet). The results of both methods are shown in the cells X6 and Z6 in the blue box above the graphs. The values are slightly different due to the different time resolutions of the files. The result of the method using the valve relay was chosen to calculate the synchronized time given in column A. In the upper graphs of the sheet the effect of the synchronization is shown, while the remaining graphs show the temperature histories in the different measuring positions.

Figure A-14: Example for the structure of fourth data sheet with temperature-records in Excel-file of experiment 20190528_104204 at $LN_2$-temperature (4 mm nozzle, 200 bar).

### Structure of the Images

The photographs taken of one experiment by camera 1 and camera 2 (typically 5-30 jpeg images per camera) are post-processed and packed in one zip-file, which is named – similarly as the Excel files - with the experiment's “date_time” stamp provided in the test matrices (see Table A-2 and Table A-3). In these tables it is indicated, for which actual test photographs are stored and published. For all temperature, pressure and nozzle diameter combination, the test documented with photographs is a relative early test and not identical with the latest test of this combination, for which the data has been stored in an Excel file. However, the experimental results do not vary for the same conditions (see reproducibility discussion below) only some sensors arrangements or measurement were changed. Therefore it was decided not to repeat the effort of taking photographs of the later experiments.

All photographs are post-processed in several steps. The most important one is the application of background oriented Schlieren (BOS) methodology. For the photographs taken with camera 1 close to the release nozzle a color BOS scheme with 7 colors was applied. The interrogation area is 8 -16 pix with a 1 pix stepping. The resolution area is 0.6 mm - 1.2 mm. Additional functions applied are a denoising, equalizing and a weight function with a 1D or 2D Gaussian sub-pixels. The color code was carefully chosen to provide best contrast for identification of the jet boundaries. Figure A-**15** shows the original picture and the result of the post-processing.

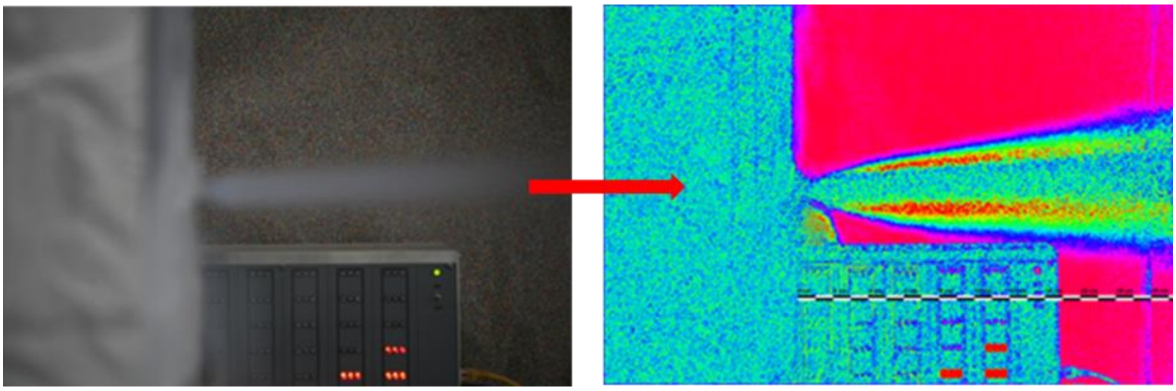

Figure A-15: Original picture and results of the color BOS post-processing of a photograph taken from the jet release with camera 1.

For the photographs taken from jet from the jet far field with camera 2, a black/white BOS scheme was applied. The interrogation area is 16 pix, 24 pix or 32 pix 8 -16 pix with a 1 pix stepping. The resolution area is 0.6 mm - 1.2 mm. Additional functions applied are a denoising, equalizing and a weight function with a 1D or 2D Gaussian sub-pixels. The color code was carefully chosen to provide best contrast for identification of the jet boundaries. Figure A-**16** shows the original picture and the result of the post-processing.

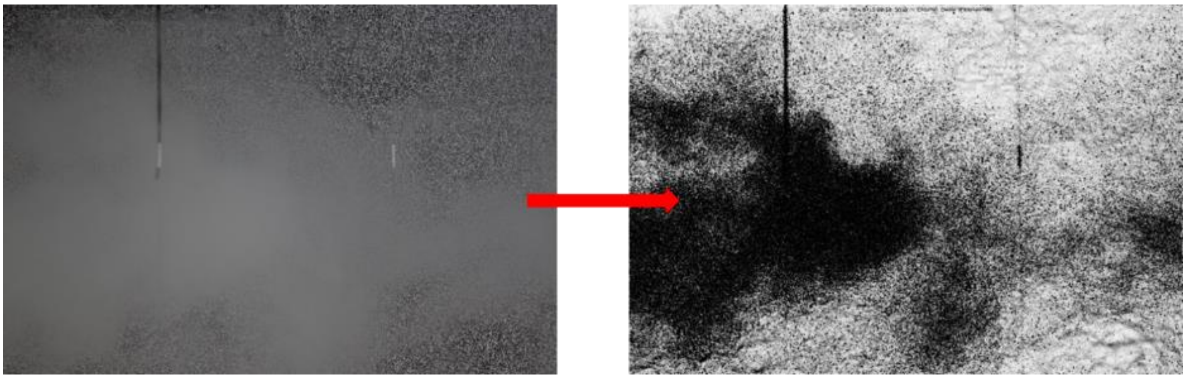

Figure A-16: Original picture and results of the black and white BOS post-processing of a photograph of the jet far field observed with camera 2.

The next figures show time sequences of original pictures taken with camera 1 and camera 2 from the near field, respectively far field of the jet release experiment 20190503_140045 (80K, 200 bar, 4 mm nozzle) and the same pictures post-processed with the corresponding BOS methods. The time 0 refers to the time of the trigger initiation.

These pictures may be retrieved from file PRE3P1A_KIT_D4_80K_PICS.zip, containing the experiment 20190503_140045 related pictures in 20190503_140045.zip. The corresponding dataset is to be found in 20190528_104204.xlsx (see Table A-3, last line, right row, entries highlighted with grey background and bold black font) in PRE3P1A_KIT_D4_80K_DATA.zip.

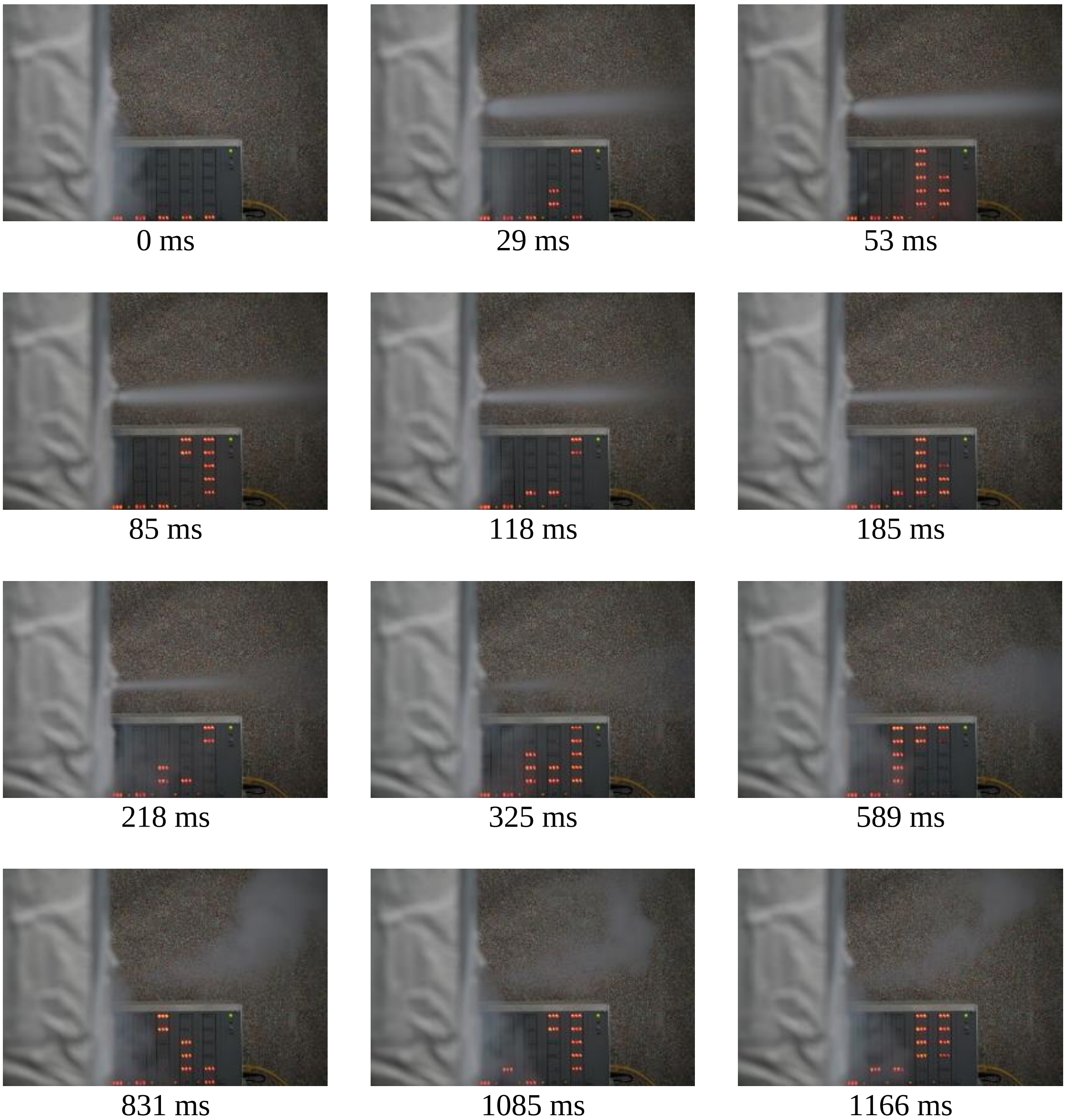


Figure A-17: Original photograph series taken from the jet release close to the nozzle (camera 1) of experiment 20190503_140045 (cold, 200 bar, 4 mm nozzle); time = 0 ms refers to the time of the trigger initiation.

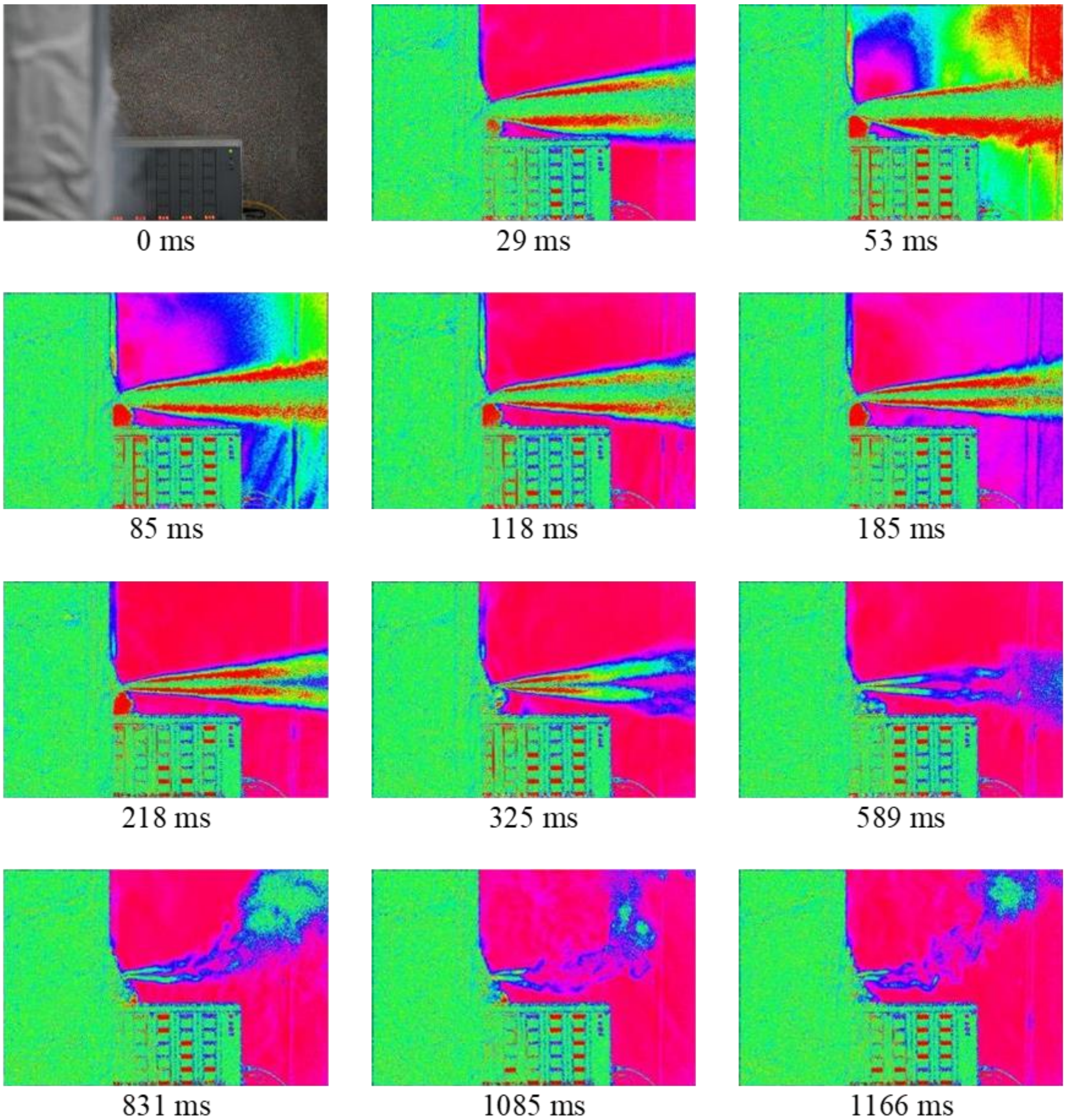


Figure A-18: Color BOS post-processed photograph series taken from the jet release close to the nozzle of experiment 20190503_140045 (cold, 200 bar, 4 mm nozzle); time = 0 ms refers to the time of the trigger initiation; the photograph at 0 ms serves as reference for the BOS procedure and therefore is “empty”.

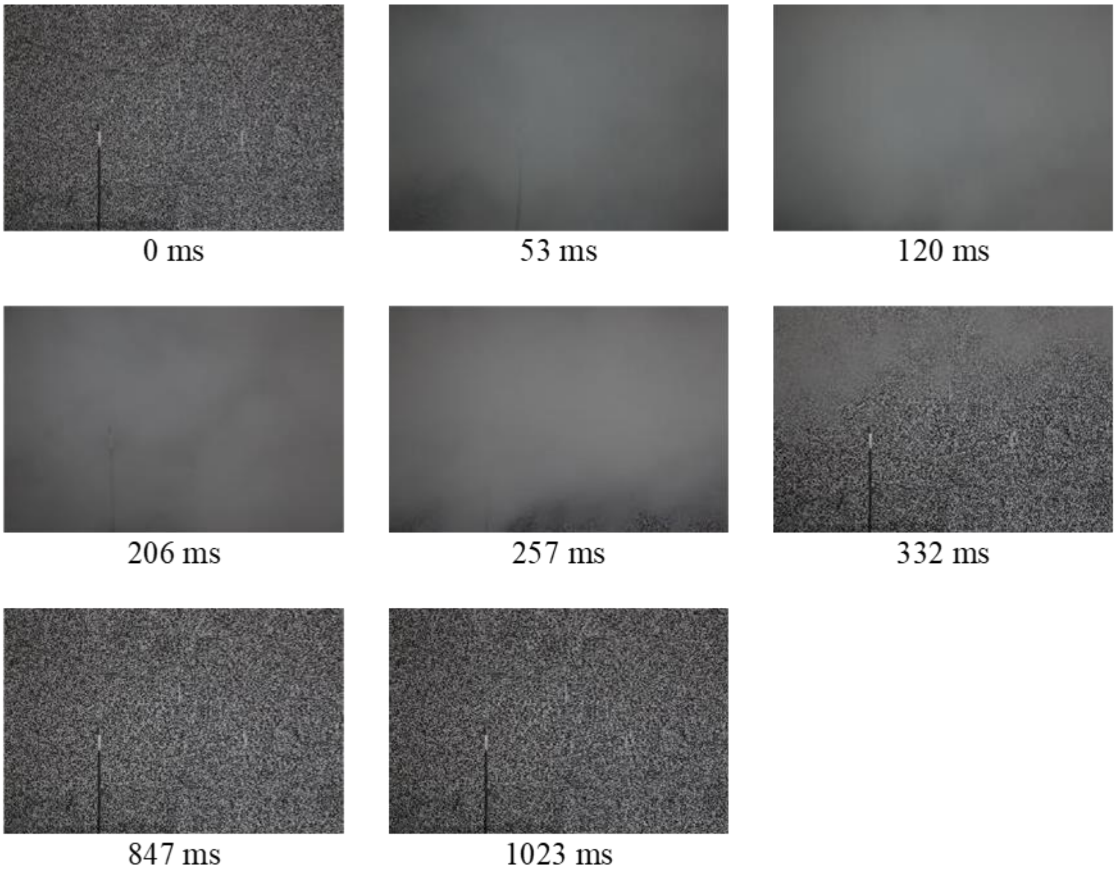


Figure A-19: Original photograph series taken from the jet far field (camera 2) of experiment 20190503_140045 (80 K, 200 bar, 4 mm nozzle); time = 0 ms refers to the time of the trigger initiation.

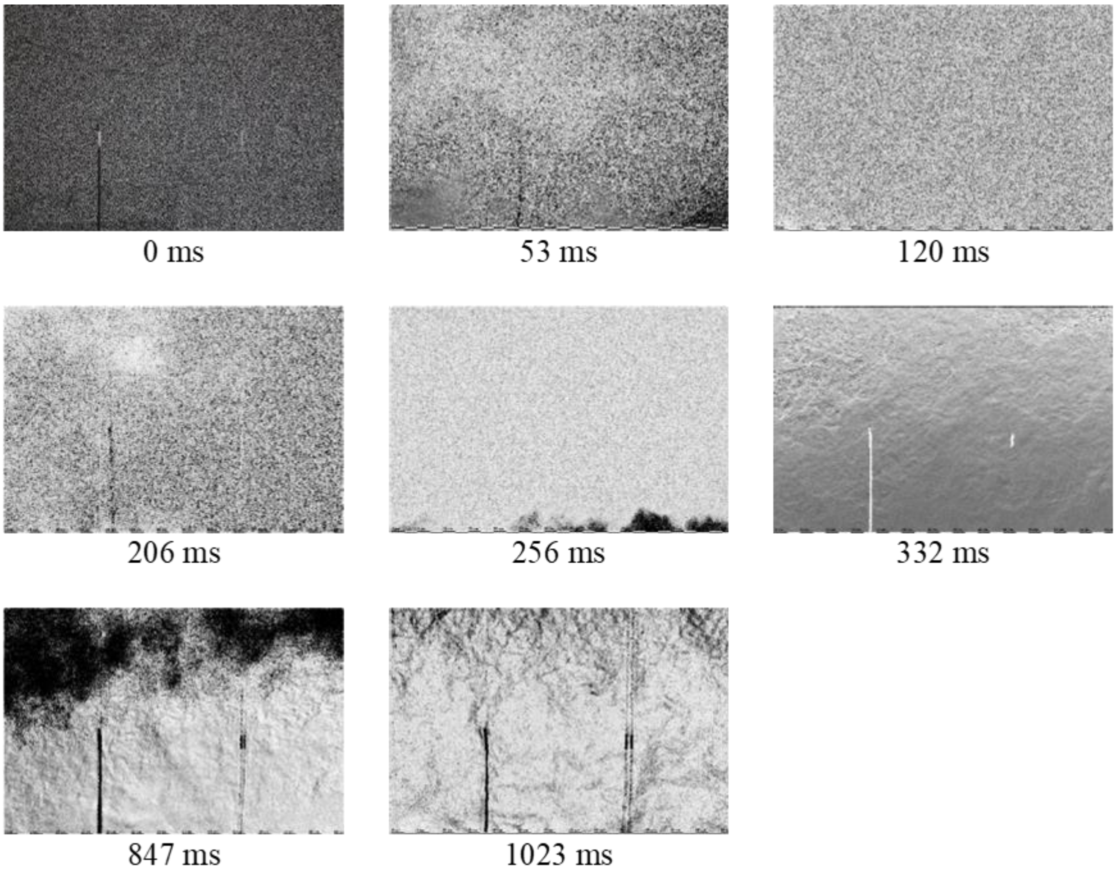


Figure A-20: Original photograph series taken from the jet far field (camera 2) of experiment 20190503_140045 (80 K, 200 bar, 4 mm nozzle); time = 0 ms refers to the time of the trigger initiation.

# Part B: Experiments in the Cyostat-Facility

## B-1 General Description of the Cryostat-Facility

Pre-calculations on the expected hydrogen mass flow for the maximum release conditions were performed and proved that the released amount of $H_2$ is too large to be handled on KIT-HyKA in case of an unintended spontaneous ignition ($P_{ini}$ = 5 bar, $d_{Noz}$ = 4 mm → $\dot{m}_{LH2}$ = 96.4 g/s), since there are several buildings with windows located in the vicinity. For this reason, the free-field test site of the Institute for Technology and Management in Construction (TMB), which is part of KIT Campus South, was loaned for the tests. This free field test site is located approx. 3.5 km north of KIT Campus North at the edge of the northern part of the Hardtwald forest (see Figure B-**1**).


Figure B-1: Location (left) and aerial view from the north (right) of the free-field test site north of KIT Campus North with later positions of the $LH_2$-trailer (blue) experimental area (red circle) and tent for data acquisition (yellow).

The biggest cost factor in the procurement of $LH_2$ for the experiments turned out to be the rental of the super-insulated trailer needed to store the $LH_2$ for the duration of all experiments with $LH_2$ at the test site. To keep these costs as low as possible it was decided to perform all experiments with $LH_2$ within a time frame that had to be held as short as possible. So the facilities for all experiments with $LH_2$ done by KIT/PS were prepared and stored at the free field test site north of KIT-Campus North before the $LH_2$-campaign began with the delivery of the $LH_2$-trailer.

The tests with the Cryostat-facility were performed on the standard location for the $LH_2$-tests on the free-field test site with the $LH_2$-trailer parked close to it besides a massive steel container and with its rear end pointing towards the experimental area. Behind the rear door of the trailer, the control panel with all valves and joint points is located and thus this door had to remain opened during the withdrawal of $LH_2$ from the trailer. For protection of this vulnerable part of the trailer a protective wall of concrete bricks (M = 500 kg/brick) was constructed between trailer and experiment. This rather crowded layout of the components was necessary due to the fact that the Cryostat-facility had to be filled with $LH_2$ from the trailer through the rather short (L ≈ 5 m) super insulated hose that was provided by Air-Liquide together with the trailer (see Figure B-**2**).


Figure B-2: Photograph of the general set-up of the Cryostat-facility.

The Cryostat facility consists mainly of a $LN_2$-shielded stainless-steel cryostat with an internal volume of 225 dm³ that was loaned for the tests from another institute at KIT. The main problem with this vessel was the missing lid with all connections, which had to be constructed and fabricated according to the needs of the experiment. The cryostat is designed for a maximum pressure of 6 bar (absolute pressure, corresponding to 5 bar overpressure). If the maximum pressure of the vessel is exceeded, an integrated safety valve opens automatically and depressurizes the facility. As further safety measure, several burst-discs are also installed. Figure B-**3** shows photographs of the Cryostat vessel and a drawing of the special lid that was fabricated for the experiments.

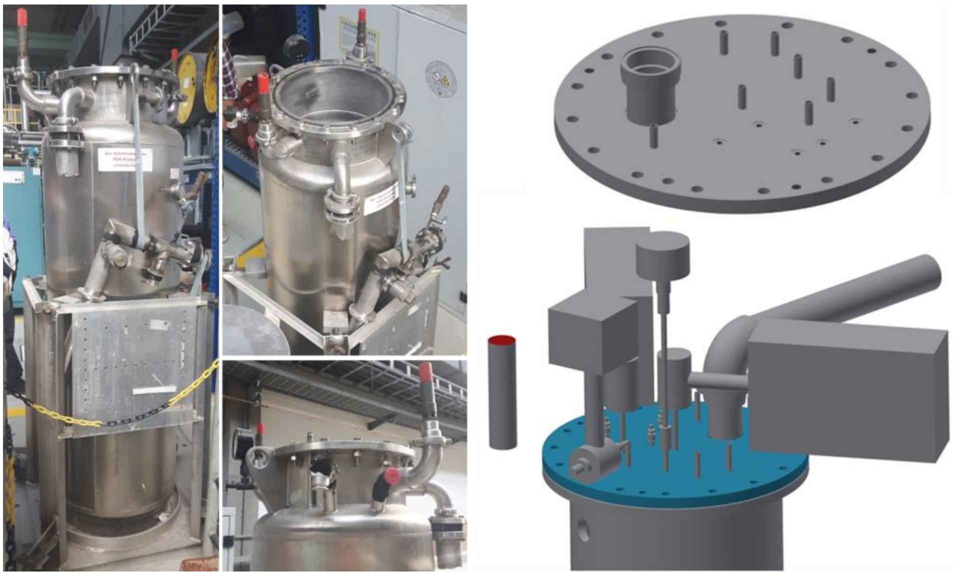

Figure B-3: Photos of the Cryostat-facility and technical drawing of the lid fabricated to house the components needed to realize a connection to the $LH_2$-trailer as well as a $LH_2$-release through the same release branch as used in the DisCha-facility.

In the special lid of the Cryostat, all components needed to realize a connection to the $LH_2$-trailer as well as a $LH_2$-release through the same release branch as used in the DisCha-facility (see Figure A-**3** and Figure B-**4**) are integrated. For the control of the filling level, a set of 5 thermocouples at different heights inside the vessel as well as a scale that measures the mass of the complete assembly can be utilized.

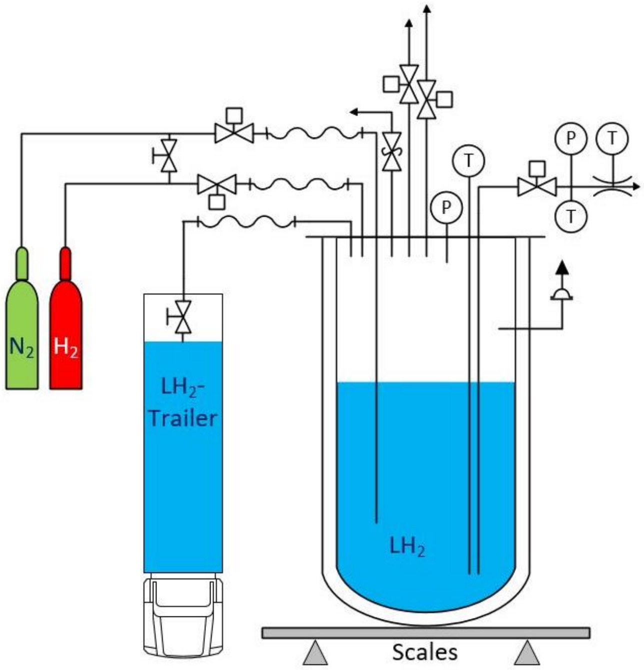


Figure B-4: Sketch of the Cryostat-facility with gas and $LH_2$-supply and instrumentation.

While in the DisCha-experiments four circular nozzle diameters were used (0.5, 1, 2 and 4 mm), in the Cryostat experiments only two of these nozzles (orifice diameter 2 and 4 mm) were used. These nozzles were the same as in the DisCha-experiments and they were also mounted to the same tubes and joints connecting them with the same release valve (Figure A-**3**). All tubes and the valve in the release branch have an inner diameter of 9 mm, while in the connectors the diameter is 9.5 mm. The complete release branch has a length of 367.4 mm from the end of the Cryostat riser duct (or the end of the release tube welded to the DisCha vessel) to the end of the nozzle orifice.

## B-2 Instrumentation of the Cryostat-Facility

### Sensors and Methods used in the Cryostat-Facility

The complete Cryostat-facility was mounted on a scale (Mettler-Toledo, Type: PFK989, range: 0 - 600 kg, Figure B-**5**) to monitor the filling level of the vessel during the filling procedure and the release experiment. Special care was taken to eliminate influences of wires and hoses. The filling level of the vessel was also monitored using 5 thermocouples that were installed inside the vessel in different heights. Similar to the DisCha-facility one pressure sensor was used to record the pressure inside the vessel throughout the complete experiment. Since the same release branch as in the DisCha-experiments is used, a second pressure sensor and a thermocouple are installed to the junction in the release line between release valve and nozzle. Both pressure sensors are the same as in the DisCha experiments (WIKA, Type: S-20, Range: 0 - 250 bar(rel.)), and also the thermocouple was unchanged since it cannot be removed from this junction.

With the Cryostat facility blowdown experiments with gaseous and liquid hydrogen were performed. During the complete series the super insulated hose from the $LH_2$-trailer was connected to its port on the lid of the cryostat. After assembly, the cryostat vessel was purged for more than one hour with gaseous nitrogen (see Figure B-**4**), before it was then purged with the gaseous boil-off hydrogen from the $LH_2$-trailer for several minutes to purge also the super insulated hose. After this the vessel was purged with gaseous hydrogen from bottles for another half an hour before the vessel was sealed and the facility was prepared for the beginning of the experimental series.

In the first series with gaseous hydrogen the cryostat vessel was filled with $H_2$ from gas bottles up to the desired pressure, with some pauses and refilling phases to achieve thermal equilibrium. After the end of this series the shield chamber of the cryostat vessel, which is insulated against the ambience and the $LH_2$-vessel by vacuum chambers, was filled with $LN_2$ to the prescribed level, while the $H_2$-pressure in the vessel was kept at a slight overpressure to eliminate air ingress from outside through potential leaks. Then the filling with $LH_2$ was initiated by purging the cryostat vessel with the gaseous boil-off hydrogen from the $LH_2$-trailer through the super insulated hose. With increasing time the flowing hydrogen becomes colder and colder before more and more $LH_2$ is purged into the cryostat vessel. During the complete filling procedure, the pressure inside the vessel is thoroughly monitored and kept at values in between 2 and 4 bar(a) to exclude air ingress and to prevent the safety devices of the vessel from opening ($p_{max}$Cryostat = 6 bar(a)). When the desired filling level (i.e. weight of complete vessel) is reached bypass valve and the $LH_2$-valve at the trailer are closed. The desired pressure in the vessel is then adjusted by cautiously adding gaseous $H_2$ from a bottle or by depressurizing through the bypass valve.

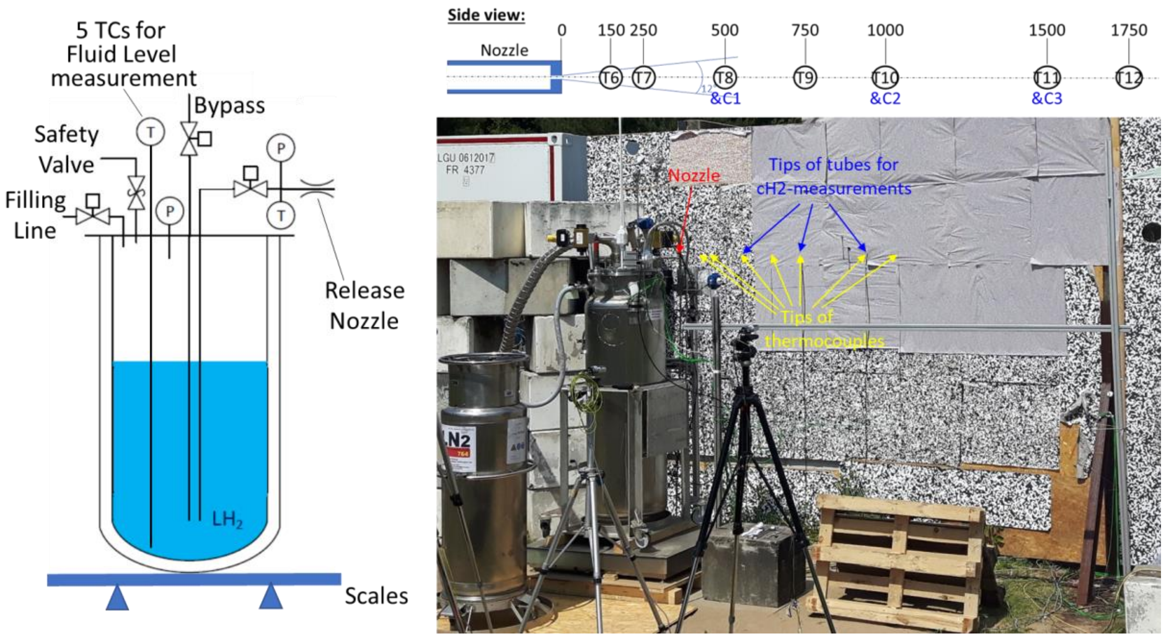


Figure B-5: Sketch and photo of the Cryostat-facility with details of the instrumentation.

Outside the release nozzle seven thermocouples and a set of three tubes for sample taking for $H_2$-concentration measurements are installed in positions on the centerline of the jet. The distances of the sensors to the release nozzle are given in Table B-**1Fehler! Verweisquelle konnte nicht gefunden werden.**.

Table B-1: Distances of the sensor positions on the jet axis to the release nozzle.

| Sensor(s) | T6 | T7 | T8 and C1 | T9 | T10 and C2 | T11 and C3 | T12 |
|---|---|---|---|---|---|---|---|
| Distance from nozzle [mm] | 150 | 250 | 500 | 750 | 1000 | 1500 | 1750 |

The seven thermocouples (Type K, diam. 1 mm, manufactured by KIT-workshop from same batch as in all other $LH_2$-experiments, compare section Estimate of Measurement Errors on next page) were positioned with their tips on the jet axis using thin metal tubes that were adjusted on a horizontal profile rail in a distance of 50 cm below the jet axis.

For the concentration measurements plastic tubes had to be used to avoid disturbances of the flow due to the bulky $H_2$-Sensors and to provide a constant gas flow from the sampling position to the sensor. The tubes had a length of 10 m and were conducted through a water bath to provide for a gas flow with almost ambient temperature since the $H_2$-sensors must not be operated with cold gas of temperatures less than -60°C. The tips of the tubes with a tilted cut were positioned on the jet axis and fastened to the metal tubes that already stabilized the thermocouples.

Three field mills (Kleinwächter EFM 1138, measuring principle influence generator) for measuring static electric field strength and five cameras (2 photo cameras (C1 and C2), 2 video cameras (P1 and P2) and 1 thermo camera (IR)) are distributed besides the cold jet to monitor the releases using the BOS-technique for the visualization of density gradients (see Figure B-**6**).

Pre-calculations of the expected hydrogen mass flow for the maximum release conditions were performed ($P_{ini}$ = 5 bar, $d_{Noz}$ = 4 mm → $\dot{m}_{LH2}$ = 96.4 g/s). It proved that the expected mass flow is too large to be measured in separate pre-tests where the effused $LH_2$ is evaporated and the gaseous flow is then measured by a flow meter at almost ambient temperature. Therefore, a scales method was chosen for mass flow measurements in which the mass of the effusing hydrogen is determined by weighing the complete facility.

To enable weight measurements the complete Cryostat-facility was placed on the scales. The total weight of the experimental set-up, as measured by the scale is about 515 kg.

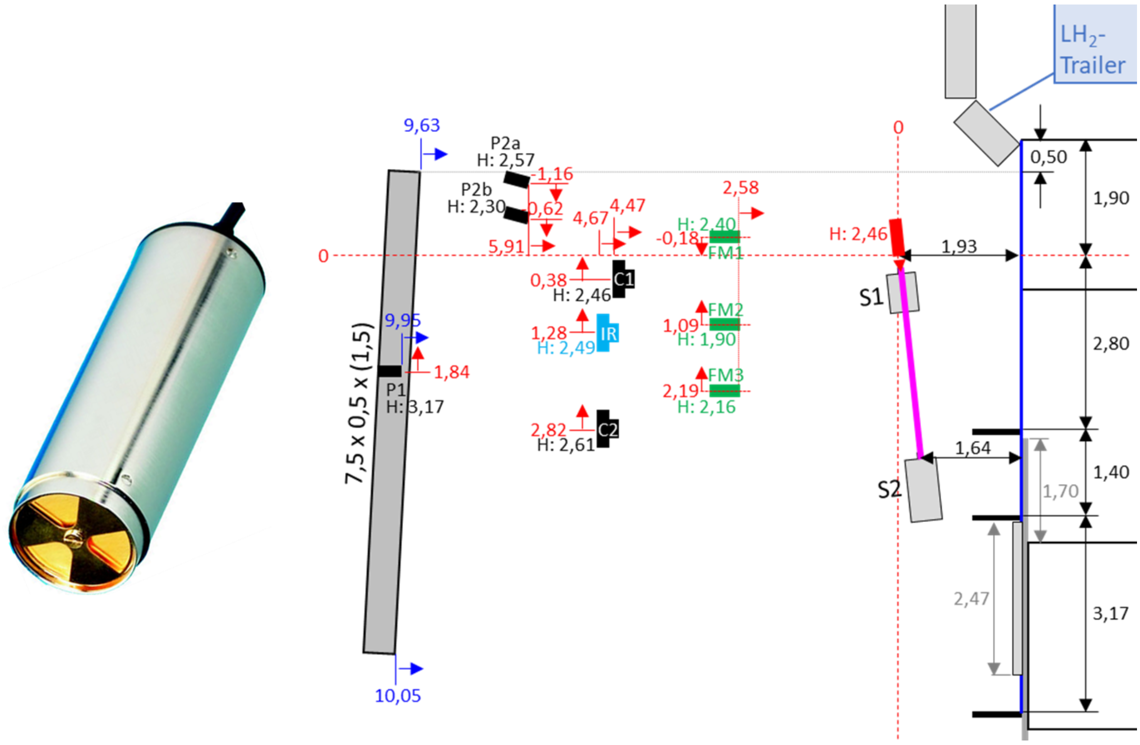


Figure B-6: Field mill of type Kleinwächter EFM 113B (left) and sketch of the Cryostat-facility with details of the instrumentation (right).

## Estimate of Measurement Errors

The accuracy of the sensors used in the experiments is given in Table B-**2** below. The values were taken from the respective manuals for ambient temperature conditions. For cryogenic temperatures no data is available. All sensors were used in both series, unless otherwise stated.

Table B-2: Accuracy of the pressure sensors, field mills and thermocouples used in the DisCha- and the Cryostat-experiments.

| Sensor | Manufacturer | Type (Range) | Non-linearity @ 290 K |
|---|---|---|---|
| Pressure | WIKA | S-20 (250 bar) | < 0,125% FS |
| Field mill | Kleinwächter | EFM 1138 (5 kV/m) | < 5% FS |
| Temperature | KIT-Workshop | Type K, d = 0.36 mm | 1.66 °C |

In the experiments neither pressure sensors nor field mills were in direct contact with the cold hydrogen, so the accuracy for ambient temperature seems to be sufficient. In contrast to this the thermocouples were exposed to the cold gas and therefore these sensors were calibrated against $LN_2$ in a pre-test and against $LH_2$ in the Pool-experiments that were conducted prior to the Cryostat-experiments. Using the three datapoints for ambient and the two cryogenic temperatures of $LN_2$ and $LH_2$ a linear dependency was formulated with which all thermocouple records were corrected. The calibration curve for the thermocouples is shown in Figure B-**7**.

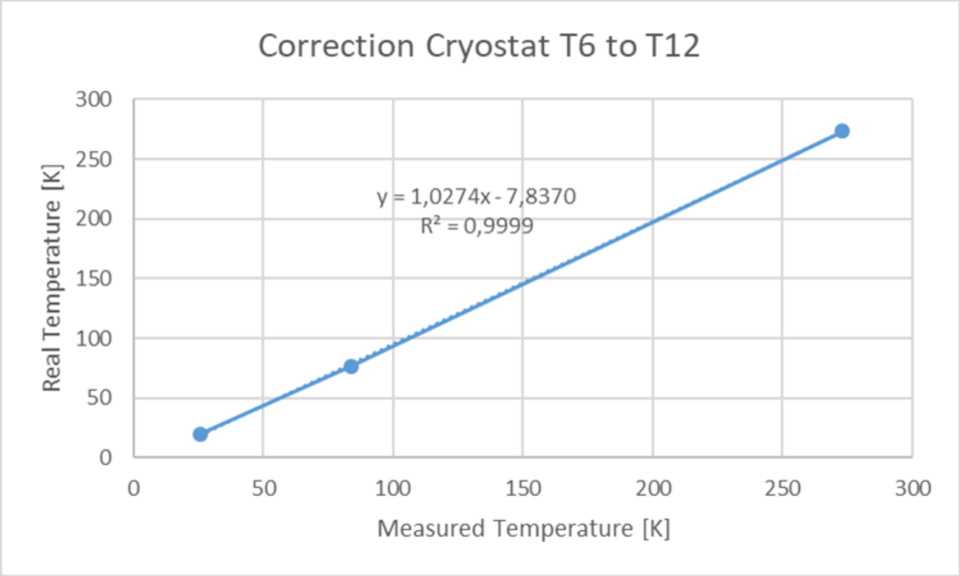


Figure B-7: Calibration curve for the thermocouples used in the Cryostat-experiments.

## B-3 Structure of Cryostat Experimental Result Data

With the Cryostat-facility 12 release experiments were performed for WP3.1b. In 7 of the tests liquid hydrogen ($LH_2$) was released from the cryostat, while in 5 reference tests gaseous hydrogen at ambient temperature was used. The Cryostat test campaign was done in May 2020 directly after the COVID19-shutdown in Germany. The first day the reference experiments at ambient temperature were made, while the cryogenic tests were performed the following day (21$^{st}$ of May 2020). In the following table for the test matrix at ambient and cryogenic temperature, a test is labeled with the date and time ("date"_"time"), at which the test was initiated:

2020**MMDD_hhmmss**

with **MM** for month, **DD** for day, **hh** for hour, **mm** for minute, **ss** for second of the formal start of the experiment. The test matrix for the blow-down experiments was compiled by varying the release nozzle diameter (two diameters: 2 and 4 mm) and the initial hydrogen storage pressure for two hydrogen storage temperature levels (two nominal storage temperatures: 30 and 290 K). Due to the limited maximum pressure of the cryostat vessel only a limited number of initial pressure levels was possible (pressure values in between 2 and 5 bar). The test matrix for the Cryostat-experiments is shown in Table B-**3**.

Table B-3: Test matrix of the Cryostat-experiments.

| | | Initial Storage Temperature [K] | | | |
|---|---|---|---|---|---|
| | | 290 | | 30 | |
| | | Nozzle-Diameter [mm] | | Nozzle-Diameter [mm] | |
| | | 2 | 4 | 2 | 4 |
| Pressure [bar] | 3,2 | 20200520_144544 | 20200520_150010 | | |
| | 4,75 | | 20200520_150332 | | |
| | 5 | 20200520_143038 | 20200520_145506 | | |
| | 2 | | | | 20200521_114818 |
| | 3,25 | | | 20200521_133851 | 20200521_111302 |
| | 4 | | | | 20200521_101847<br>20200521_121012 |
| | 4,25 | | | 20200521_125654 | |
| | 4,5 | | | | 20200521_113404 |
| Folder | | Sheet | | Sheet | |
| **PRE4P2_KIT_ Cryostat_ Dall_290K** | | **20200520-290K 2mm**<br>**20200520-230K 4mm** | | | |
| **PRE4P2_KIT_ Cryostat_ Dall_30K** | | | | **20200521-30K 2mm**<br>**20200521-30K 4mm** | |

As displayed in the lower part of Table B-**3** the data of the experiments is stored in four folders corresponding to the two nominal initial temperatures and the two nozzle diameters used.

In the folders two Excel-files are present for every experiment. The first, with the extension “PFast-Cut”, contains the data of the two pressure sensors in the vessel and the nozzle as well as the trigger-signal in its original frequency of 1000 Hz (Figure B-**8**).

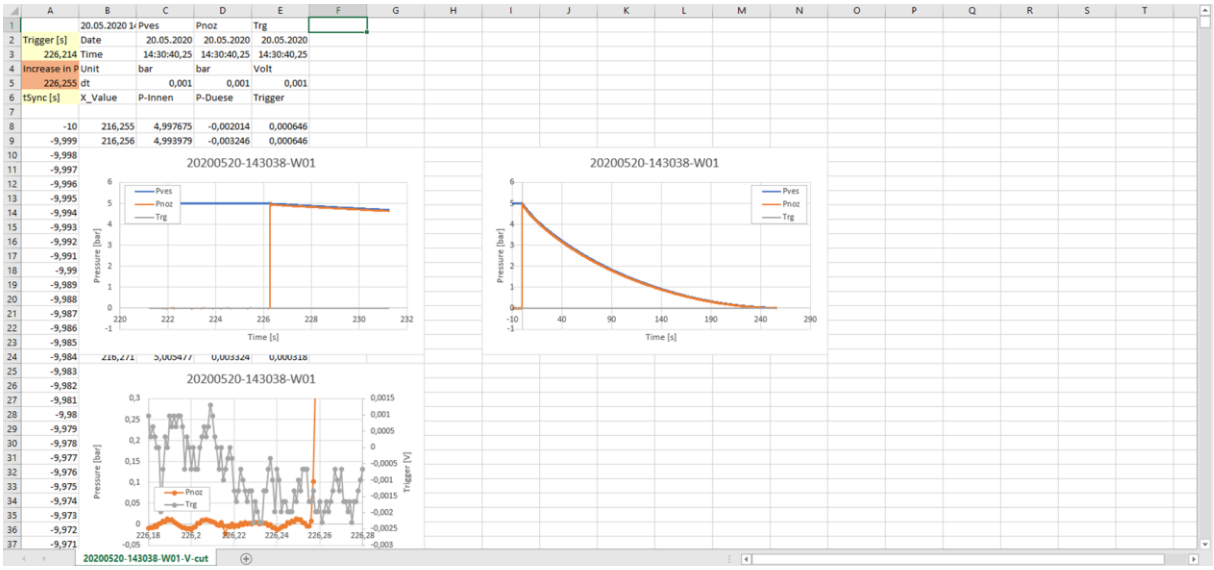

Figure B-8: Data sheet with high-resolution pressure records.

Due to the enormous size of this record the data is tightly cut (10 s pre-trigger and approx. 20 s after end of release). The time scale is corrected in a way that the first pressure increase in the release nozzle corresponds with the time “0” of the synchronized time scale. This correction was done to provide the same time-scale for all data of all devices used in the experiments.

For the rest of the data, it was found worthwhile to reduce the amount of data by decimating it by a factor of 10. So in the second data file with the extension “Final” the sensor signals recorded together with the pressure sensors are stored with a reduced frequency of 100 Hz on the first sheet with the extension “VD10” (Figure B-**9**).

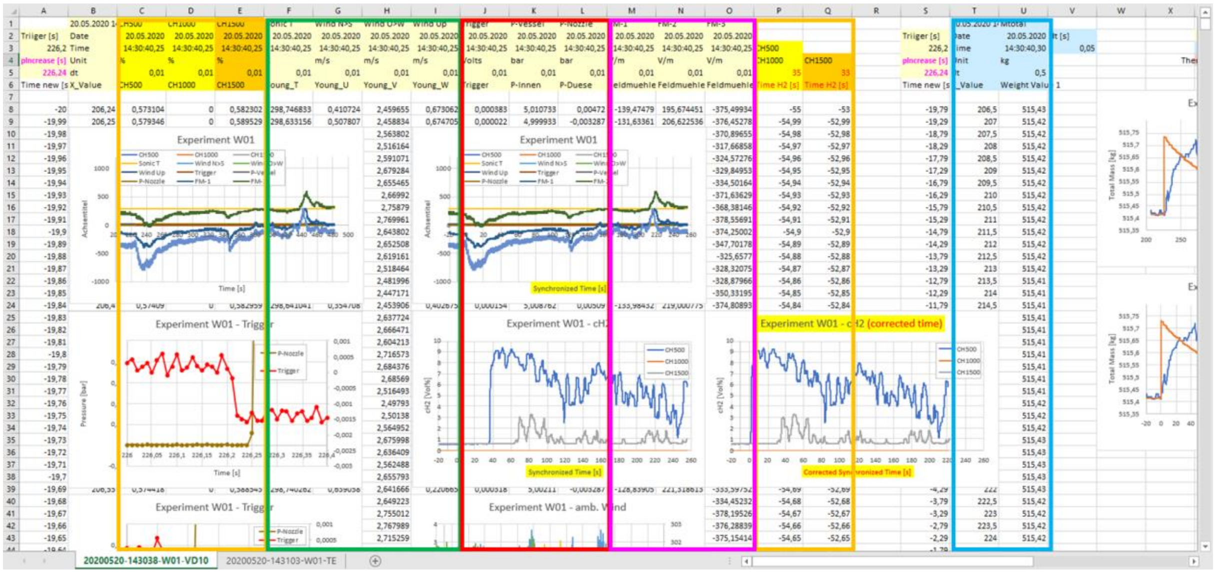

Figure B-9: Data sheet with pressure records and other sensor signals in lower resolution.

Apart from the pressure and trigger-signals (red rectangle in Figure B-**9**) also the ambient conditions (sonic temperature and wind measured by the anemometer, green rectangle) as well as the $H_2$-concentration measurements are listed (left orange rectangle). Due to the long cannulas needed for the concentration measurements separate time scales for the three sensors are given at the right end of the data block (right orange rectangle). Three further columns give the values measured by the field mills during the experiments (magenta rectangle). As separate data column at the right end of the sheet the signal of the scales, measuring the mass of the complete assembly is listed (blue rectangle). The time scale for all columns is synchronized in a way, that the first increase in the signal of the pressure sensor in the nozzle corresponds to the time “0”.

In the second data sheet (extension “TE”) all temperature measurements are listed as original data (left) and as corrected values (right) after being corrected with the procedure described above (Figure B-**10**).

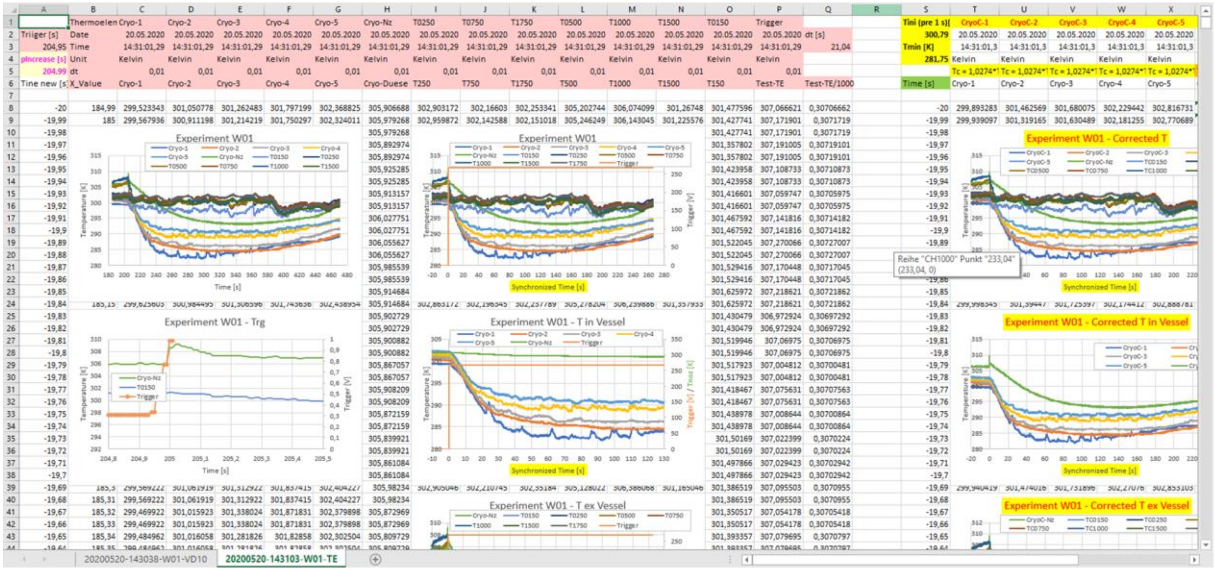


Figure B-10: Data sheet with the original temperature records (left) and corrected signals (right) using the equation presented in Figure B-7.

# Part C: Some General Observations

In the frame of the E3.1 Part A test series of the PRESLHY project 224 hydrogen blow-down experiments were made and evaluated using the DisCha-facility of KIT. 98 of the experiments were made at cryogenic temperatures, close to the standard boiling temperature of nitrogen (approximately 80 K) and 126 at ambient temperature (approximately 300 K). The measurement of pressure, temperature and concentrations in the pressure vessel and in the released jet was steadily. After the first two days of experiments, for instance, a fast pressure measurement was added ($4^{th}$ raw data file), since it was found that the frequency used initially was far too slow. Further sensors were added (additional open thermocouples, field mills) and a signal corresponding to the activation of the release valve was added for a more accurate synchronization of the different data files recorded.

The inventories stored in the DisCha pressure vessel for those blow-down experiments vary from about 1,2 g, for the lowest pressure 5 bar and ambient temperature, to about 140 g, for the highest pressure 200 bar and standard boiling temperature of nitrogen. Table C-1 contains the densities for the relevant conditions and the corresponding inventories in the DisCha vessel with 2.815 $dm^3$ free volume. The densities have been derived with real gas factors extracted from [2].

Table C-1: Hydrogen inventories of the DisCha experiments.

| **Temperature / K** | **Pressure / bar** | 1 | 5 | 10 | 20 | 50 | 100 | 150 | 200 |
|---|---|---|---|---|---|---|---|---|---|
| **293,15** | Ideal Density / (g/l) | 0,083 | 0,414 | 0,827 | 1,654 | 4,136 | 8,271 | 12,407 | 16,542 |
| | Z -factor @ 300 K | 1,000 | 1,000 | 1,008 | 1,013 | 1,030 | 1,060 | 1,090 | 1,120 |
| | **Density / (g/l)** | 0,083 | **0,414** | **0,821** | **1,633** | **4,015** | **7,803** | **11,382** | **14,770** |
| | **H2 mass in DisCha / g** | 0,233 | **1,164** | **2,310** | **4,597** | **11,303** | **21,966** | **32,042** | **41,578** |
| **77** | Ideal Density / (g/l) | 0,315 | 1,574 | 3,149 | 6,298 | 15,745 | 31,490 | 47,235 | 62,980 |
| | Z -factor @ 80K | 1,000 | 0,990 | 0,980 | 0,970 | 0,960 | 1,020 | 1,130 | 1,260 |
| | **Density / (g/l)** | 0,315 | **1,590** | **3,213** | **6,493** | **16,401** | **30,872** | **41,801** | **49,984** |
| | **H2 mass in DisCha / g** | 0,886 | **4,477** | **9,045** | **18,277** | **46,169** | **86,906** | **117,669** | **140,704** |

Even for the experiments with highest inventory - e.g. for experiment 20190528_104204, which is used for the further discussions - the weight and the repulsive force measurements show perturbations and limited precisions, see Figure C-**1**. So, these data should be considered rather qualitative than quantitative.  Best quality is provided in the pressure recordings.

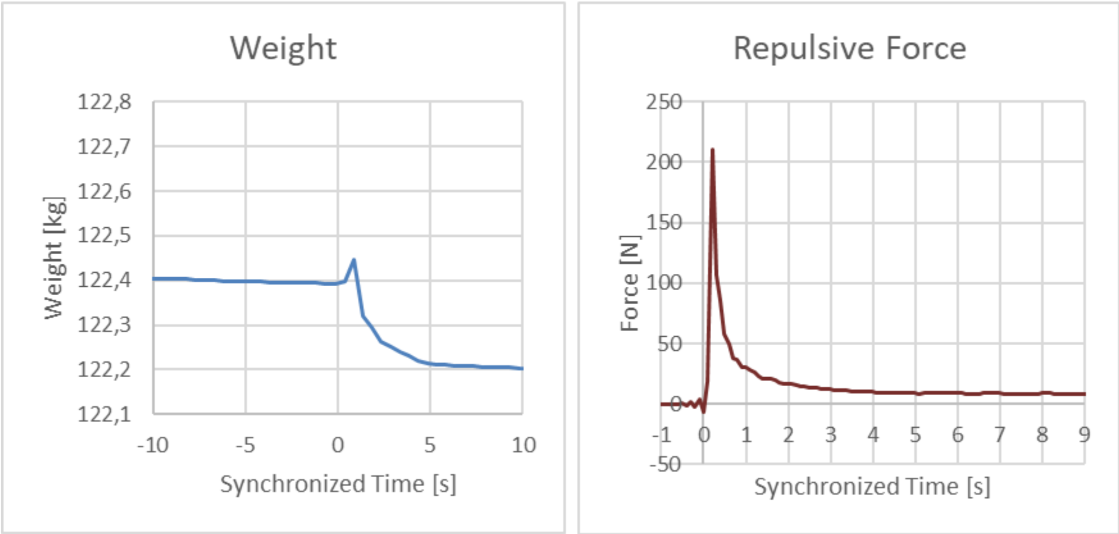


20190528_104204 (4mm, 200 bar, $T_{LN2}$)

Figure C-1: Weight and repulsive force measurements of the DisCha set-up for hydrogen blow-down starting with 200 and nitrogen boiling temperature

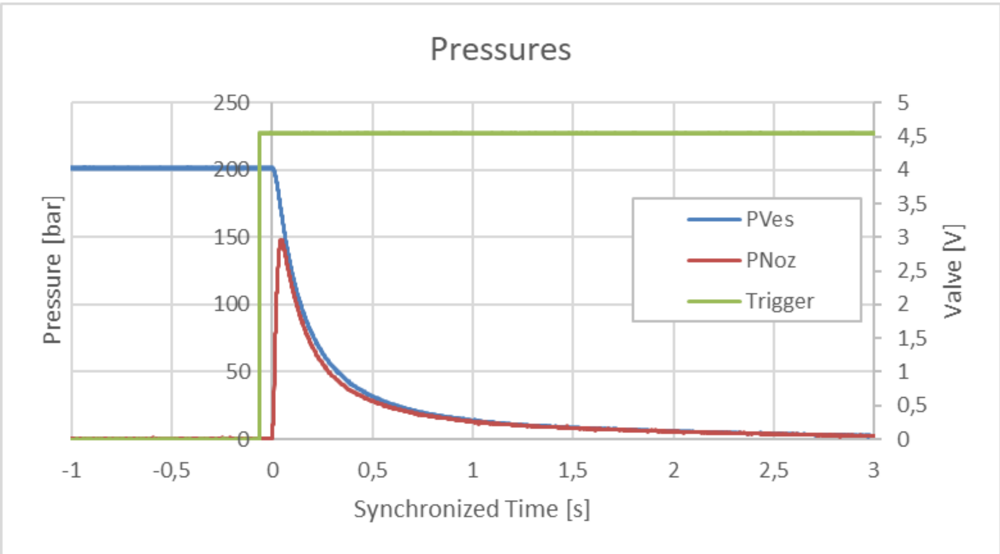


20190528_104204 (4mm, 200 bar, $T_{LN2}$)

Figure C-2: Pressure measurements in the vessel and release line before the nozzle and trigger signal for hydrogen blow-down starting with 200 and nitrogen boiling temperature

As explained above all experiments with identical temperature, pressure and nozzle diameter combination have been repeated at least three times (with the only exception of the cold test with 100 bar and 1 mm nozzle diameter). The test series with 4 mm nozzle at ambient temperature with a pressure of 100 bar provide 8 and the 200 bar 7 repetitions and allow for a statistical evaluation of the measured reservoir pressure. The root-meansquare deviation (RMSD) for the two test series was calculated and for 100 bar it is less than +/- 0.5%. For 200 bar it is about +/- 1%. Figure C-**3Fehler! Verweisquelle konnte nicht gefunden werden.** qualitatively demonstrates the good reproducibility of these experiments by plotting all 7 curves and their averages in an overlay mode in the same diagram.

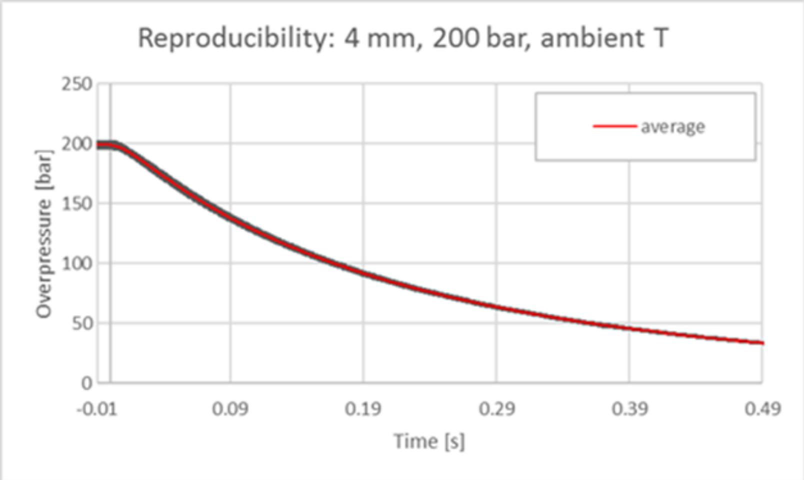


Figure C-3: Qualitative demonstration of the reproducibility of the 200 bar blow-down experiments of hydrogen with ambient temperature (RMSD of vessel overpressure 1%)

Although the actual further exploitation of the data, like determination of discharge coefficients and modelling of electrostatic field generation, is left for the further work in the PRESLHY work packages WP3 and WP4, some observations should be presented already here:

- Not a single test showed a spontaneous ignition, although
- The tests done with hydrogen at ambient temperature do not generated any significant electrostatic field, whereas the cold jets generate relative strong static electricity, in the order of 5 kV/m (see Figure C-**4**). This is 100 - 1000 times stronger than the natural electrostatic background field. The strong static electricity seems to be generated by ice crystals (potentially water ice from ambient humidity) which form on the release nozzle before the tests. The jet entrained electric charge is in some cases positive in other cases negative. These findings are supported by similar pre-cursor experiments done in the KIT test cell.
- In all cold tests white fog was generated in the jet domain. It is assumed that this mainly attributed to the ambient humidity, which condensates in the cold entrainment zone. The weather conditions for late April to early June at the experimental site (KIT Campus North) had a minimum relative humidity of 35% at 32°C, experiments in the afternoon of 4 June 2019, and a maximum humidity of almost 100% in the morning of 9 May 2019.
- The cold tests with large diameter and high pressure show strong temperature decay in the reservoir (see Figure C-**5Fehler! Verweisquelle konnte nicht gefunden werden.**) and a quite strong fog generation. However, as stated above it is currently assumed, that these particles are water droplets and ice crystals from ambient humidity. The latter originate at least partially from ice crystals formed on the

nozzle before the actual test. It may not be excluded that there is involved condensation of other gases, like CO2, oxygen or even hydrogen, as the acceleration during the release might bring down the dynamic temperature even below the hydrogen boiling point. Only detailed multi-phase simulations accounting for non-equilibrium effects might clarify this issue.

- The fog generated impaired the BOS methodology, in particular in the far field measurements.

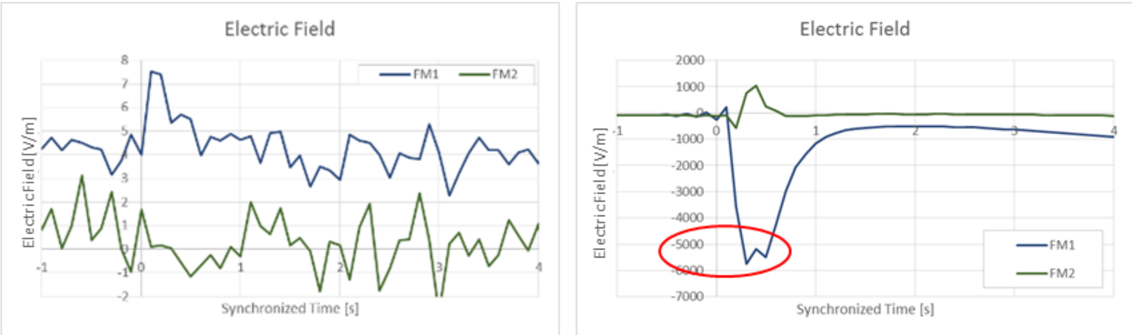


20190523_113015 (4mm, 200 bar, ambient T)

20190528_104204 (4mm, 200 bar, $T_{LN2}$)

Figure C-4: Electrostatic field measured with field mills FM1 and FM2 for blow-down of 200 bar hydrogen at ambient temperature (left) and at standard nitrogen boiling temperature (right)

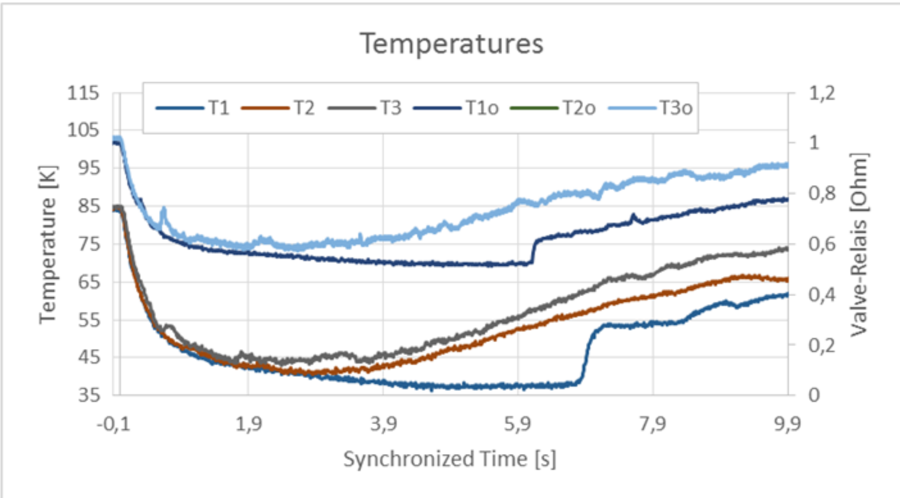


20190528_104204 (4mm, 200 bar, $T_{LN2}$)

Figure C-5: Temperature measurements in the DisCha vessel for blow-down of 200 bar hydrogen starting from standard nitrogen boiling temperature (measured 84 K on T1, T2 and T3 correspond to 77 K)

## Summary, Conclusions and Outlook

In the frame of the PRESLHY project more than 200 hydrogen blow-down experiments were made with the DisCha-facility at KIT, about half of them were made at ambient temperature, the other half at cryogenic temperatures, approximately 80 K. The reservoir pressure has been varied from 5 to 200 bar, the tested release nozzle diameter was 0.5, 1, 2 and 4 mm. Extensive equipment was used to measure hydrogen mass, pressure and temperature in the pressure vessel and temperature, hydrogen concentration and electrostatic field in and around the released gas jet. Additionally, all ambient conditions, like temperature, pressure and relative humidity have been recorded. From representative experiments photographs of the near field and far field of the released gas jet were taken and post-processed applying different BOS schemes. From a slightly more remote point movies were recorded.

During the experimental campaign the facility was continuously improved and extended, since several problems with the facility and instrumentation were encountered. The tests have been repeated for each parameter combination 3 to 8 times and the measured variables, in particular the pressure signals show very good reproducibility. The sub-set of the generated experimental data providing best measurement quality and the corresponding series of photographs will be published via KITopen [1].

The results will be used for discharge coefficient calculations, cryogenic jet and ignition modelling and for proper preparation of the ignited versions of the same tests, representing the combustion/jet fire test series E5.1. However, for those ignited tests the DisCha facility had to be moved to a remote location for safety reasons. The experiments are expected to start this summer.

The discharge tests using a liquid hydrogen container - representing the part B of the E3.1 test program - are under preparation. They will examine the two-phase effects of the discharge at moderate pressures, up to 5 bar. This pressure is the low end of the pressure applied here and therefore there is a good opportunity for comparing and linking the outcomes of part A and part B of the blow-down experiments E3.1.

## References

[1] KITopen, public research data repository; link for datasets and this report: https://doi.org/10.5445/IR/1000096833

[2] McCarty, R.D., Hord, J., and Roder, H.M. Selected properties of hydrogen (engineering design data). Final report. United States: N. p., 1981. Web.

# Appendix A1: Result Diagrams of Experiment 20190528_104204 (80K, 4mm, 200 bar)

## Diagrams in 20190528_104204-Press

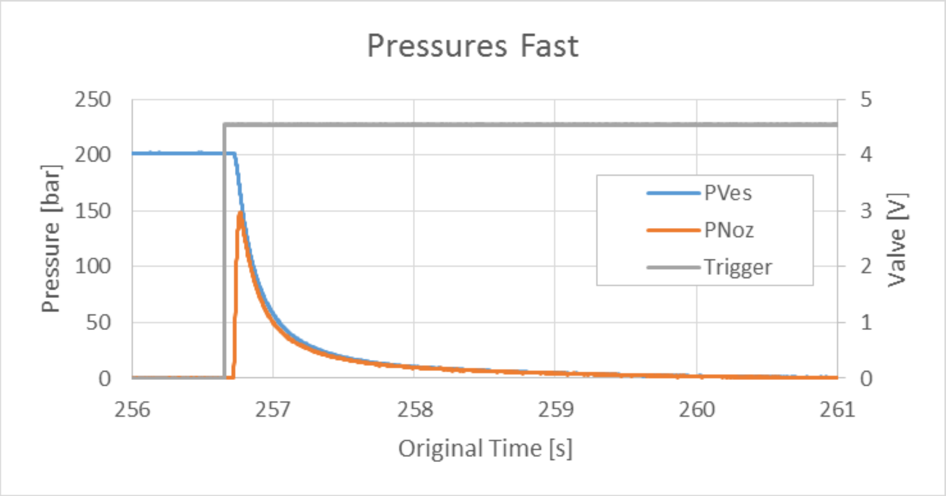


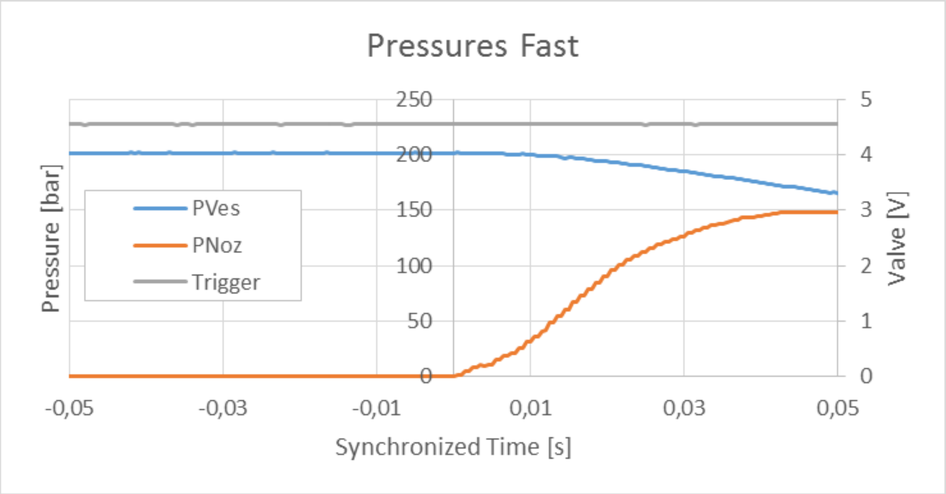


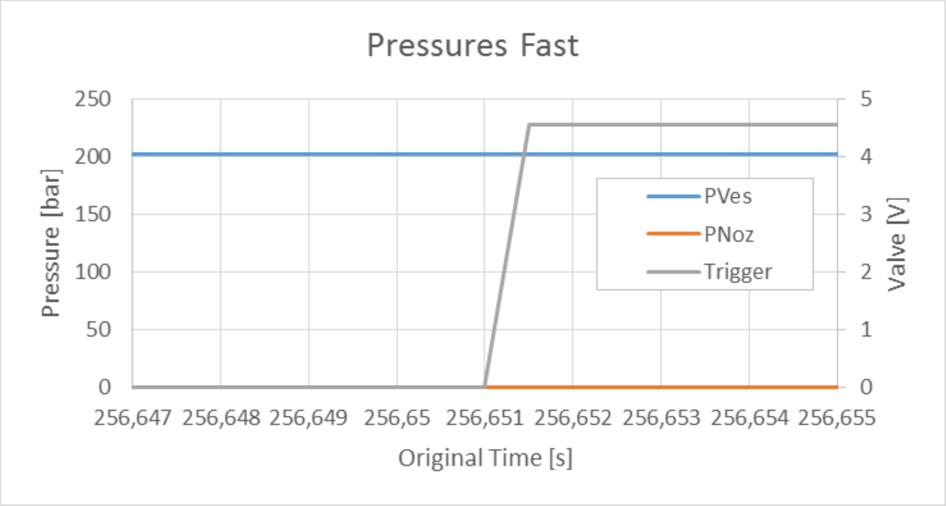

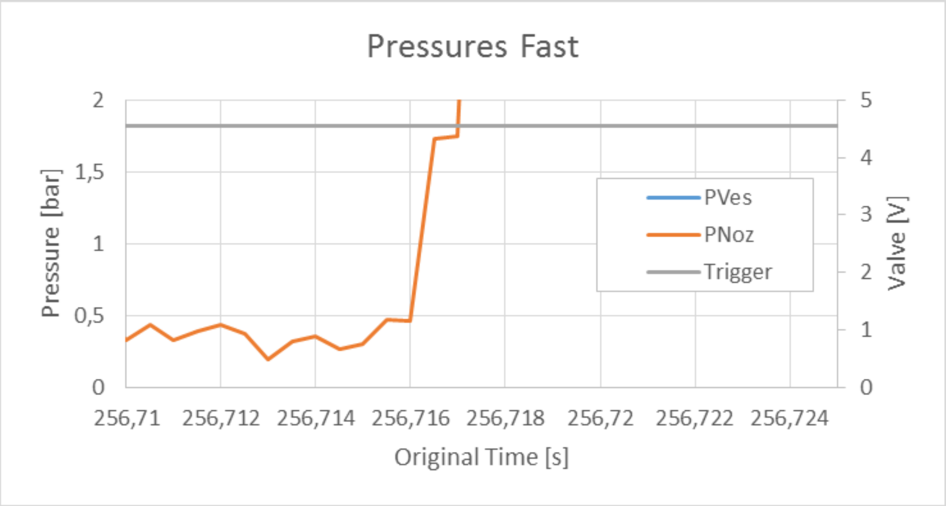
Pressures Fast
Pressure [bar]
Valve [V]
PVes
PNoz
Trigger
Original Time [s]
256,71
256,712
256,714
256,716
256,718
256,72
256,722
256,724

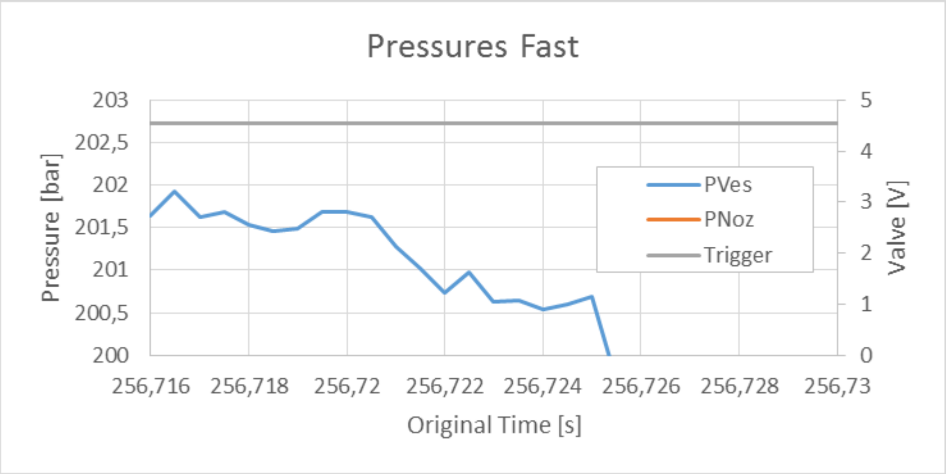
Pressures Fast
Pressure [bar]
Valve [V]
PVes
PNoz
Trigger
Original Time [s]
256,716
256,718
256,72
256,722
256,724
256,726
256,728
256,73

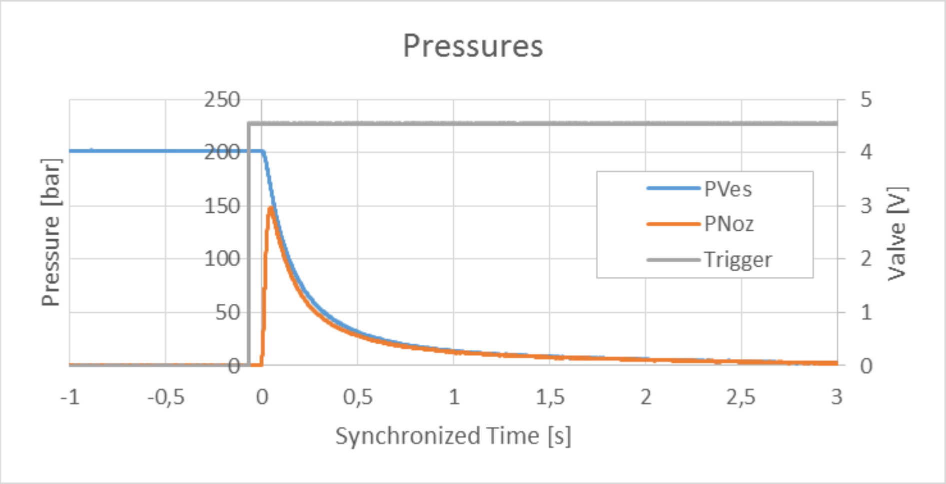
Pressures
Pressure [bar]
Valve [V]
PVes
PNoz
Trigger
Synchronized Time [s]

## Diagrams in 20190528_104204-cH2-Amb

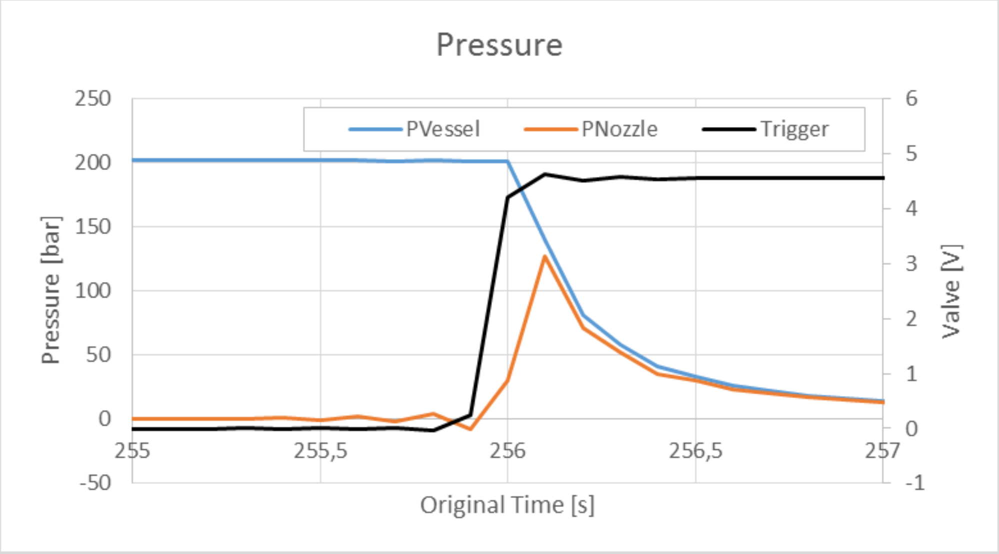


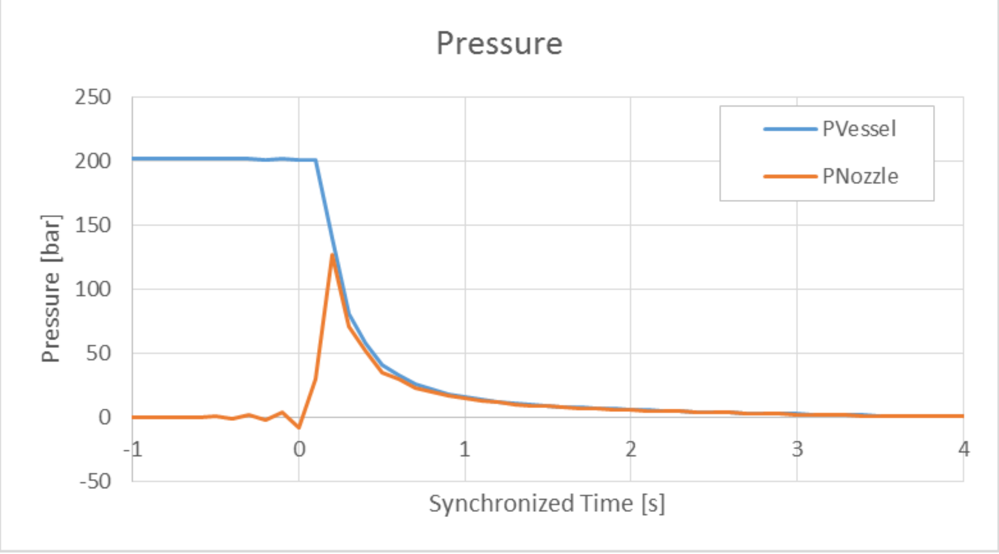


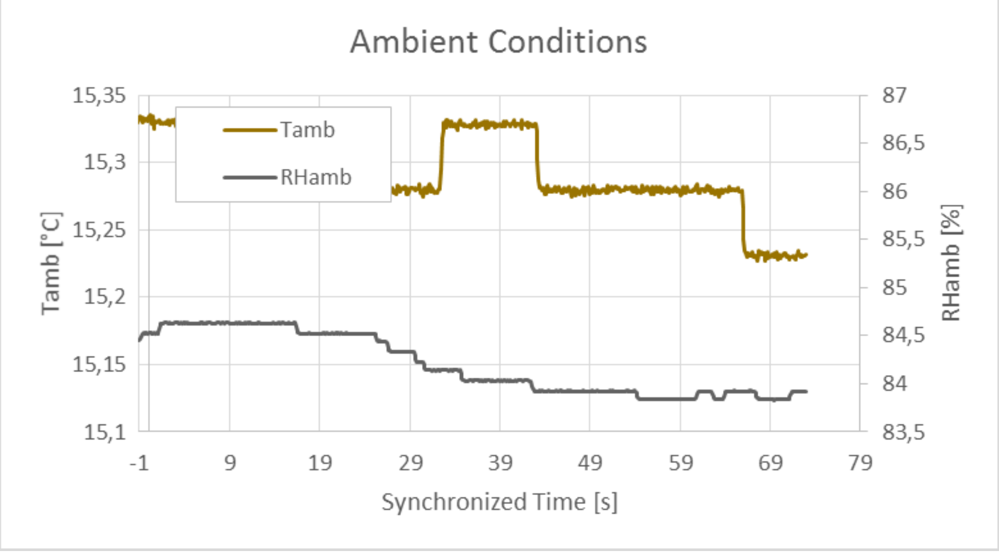

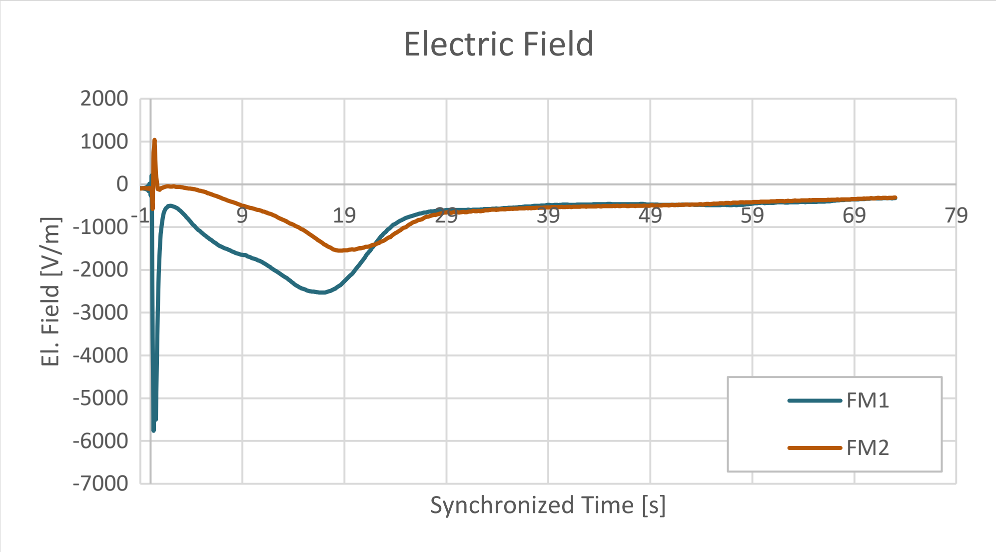
Electric Field
El. Field [V/m]
Synchronized Time [s]
FM1
FM2

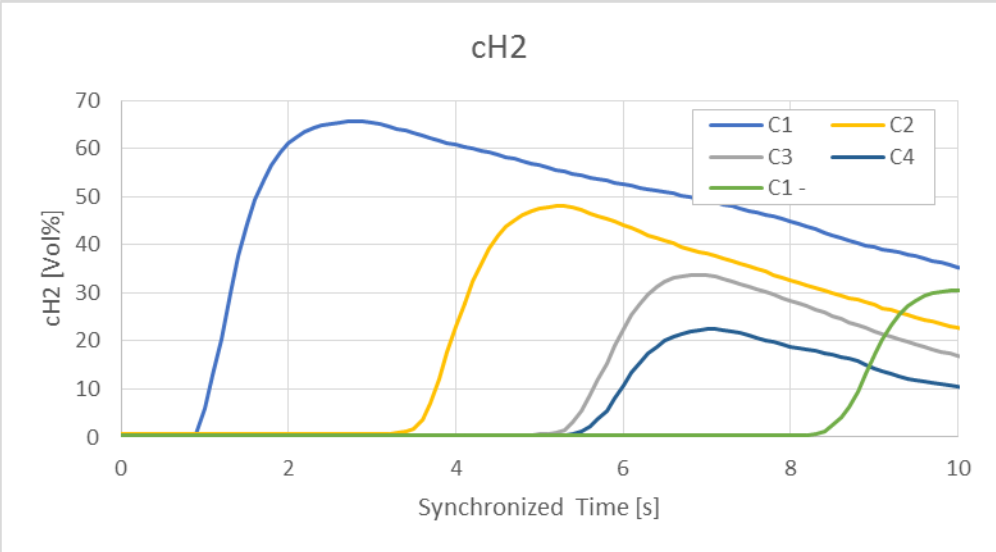
cH2
cH2 [Vol%]
Synchronized Time [s]
C1
C2
C3
C4
C1 -

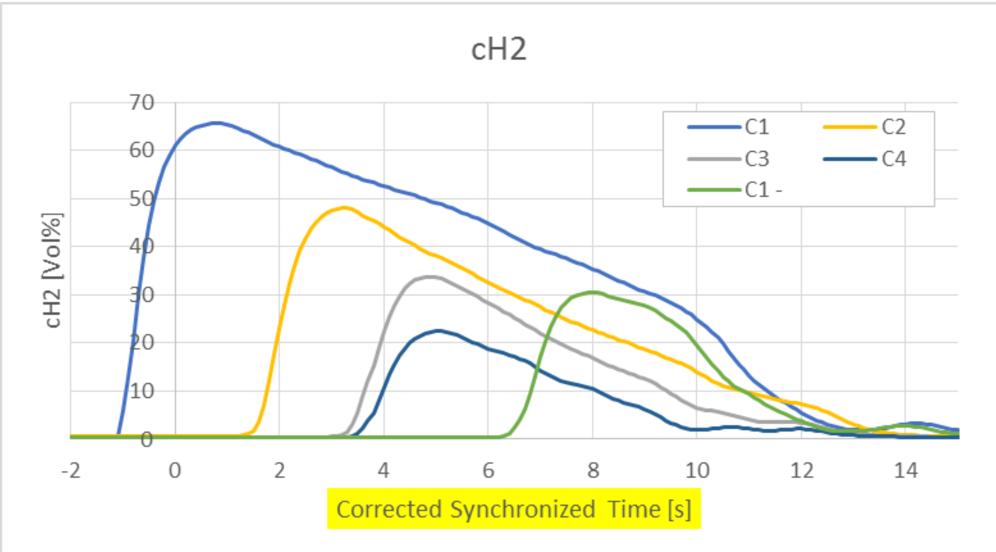
cH2
cH2 [Vol%]
Corrected Synchronized Time [s]
C1
C2
C3
C4
C1 -

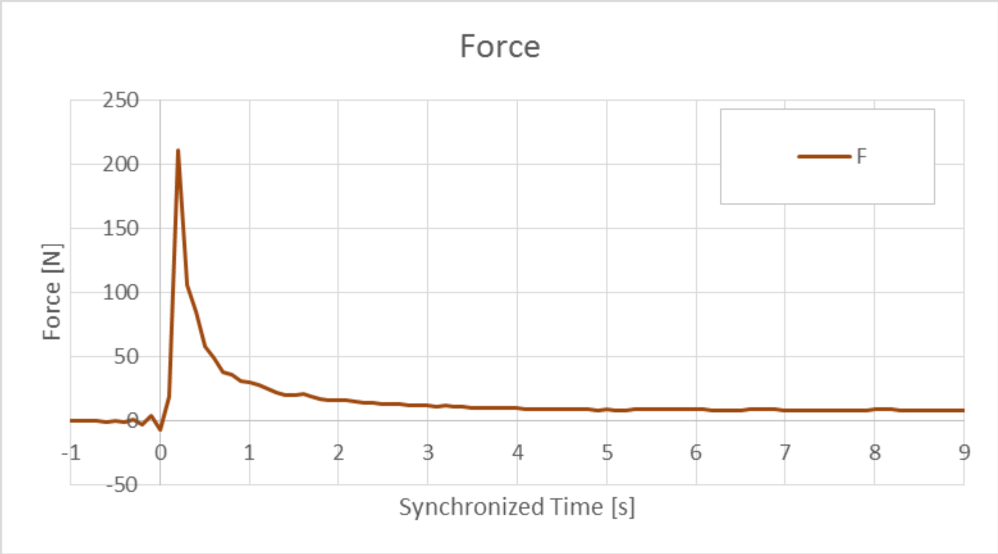
Force
250
200
150
100
50
0
-50
-1
0
1
2
3
4
5
6
7
8
9
Force [N]
Synchronized Time [s]
F

## Diagrams in 20190528_104204-Weight

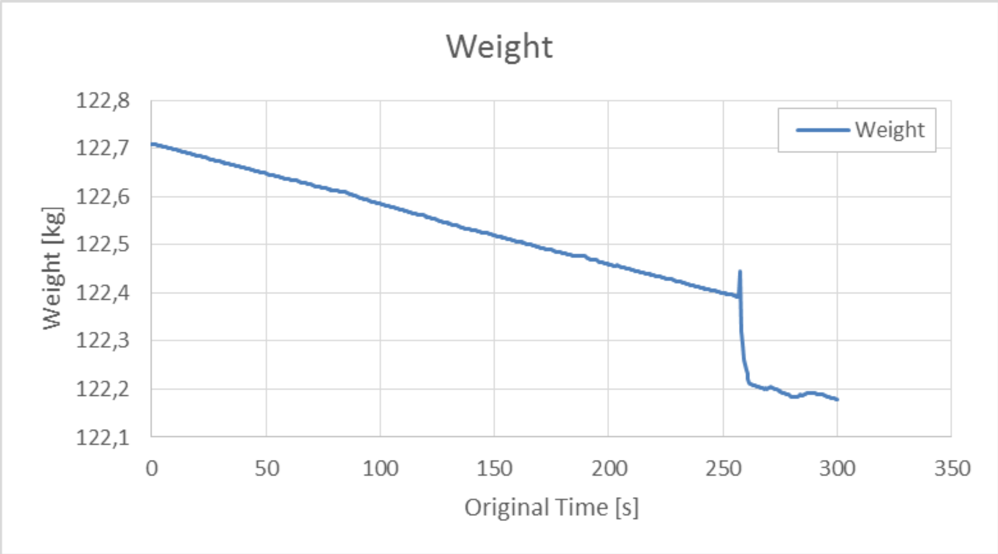


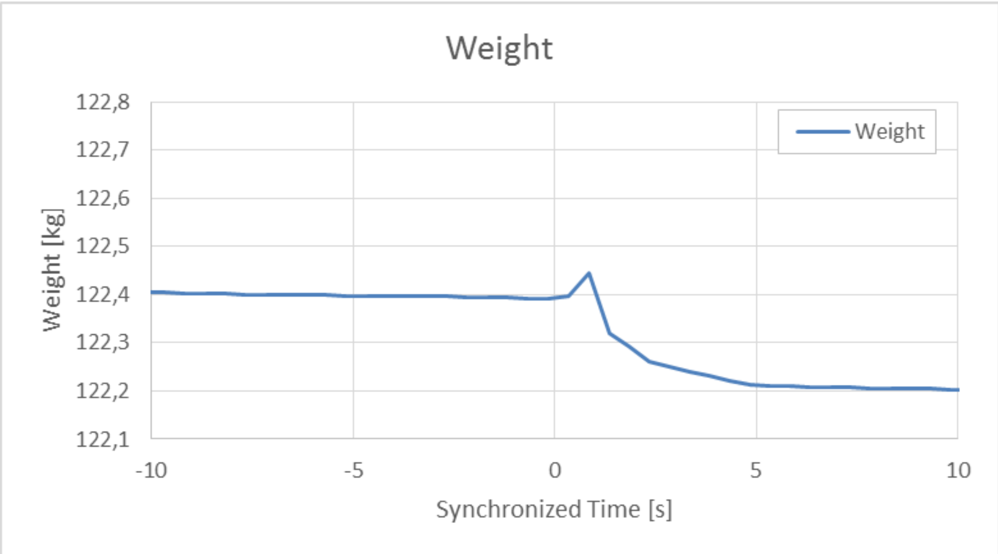

## Diagrams in 20190528_104218-Temp

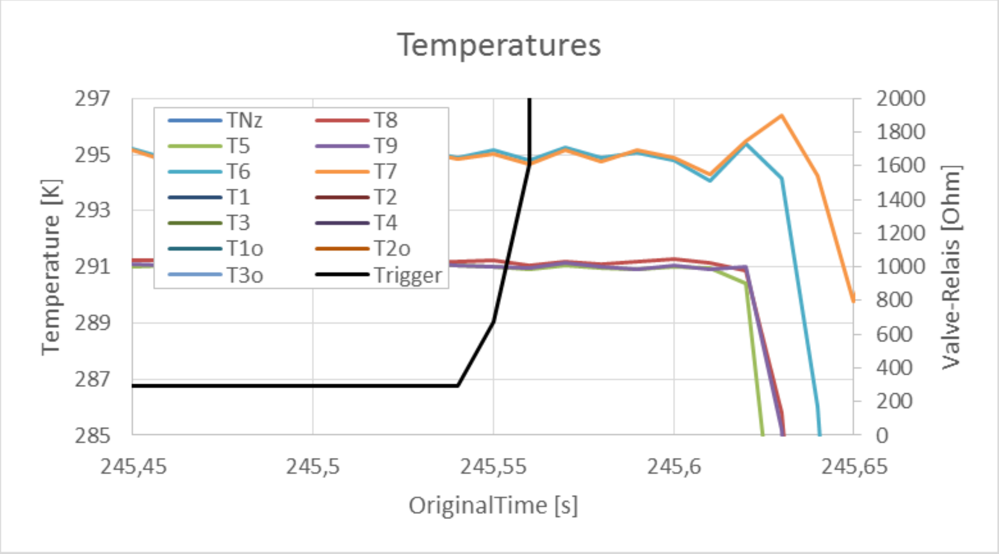


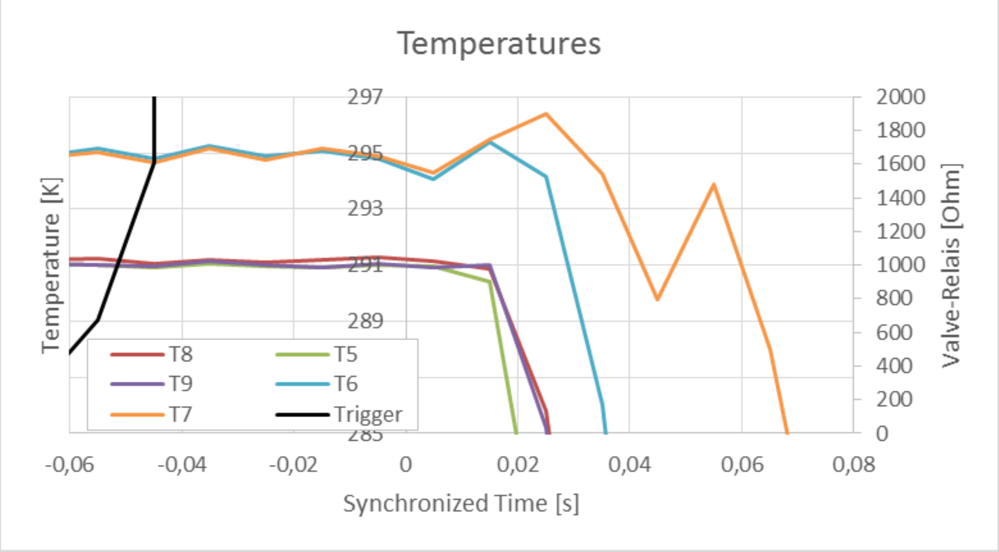


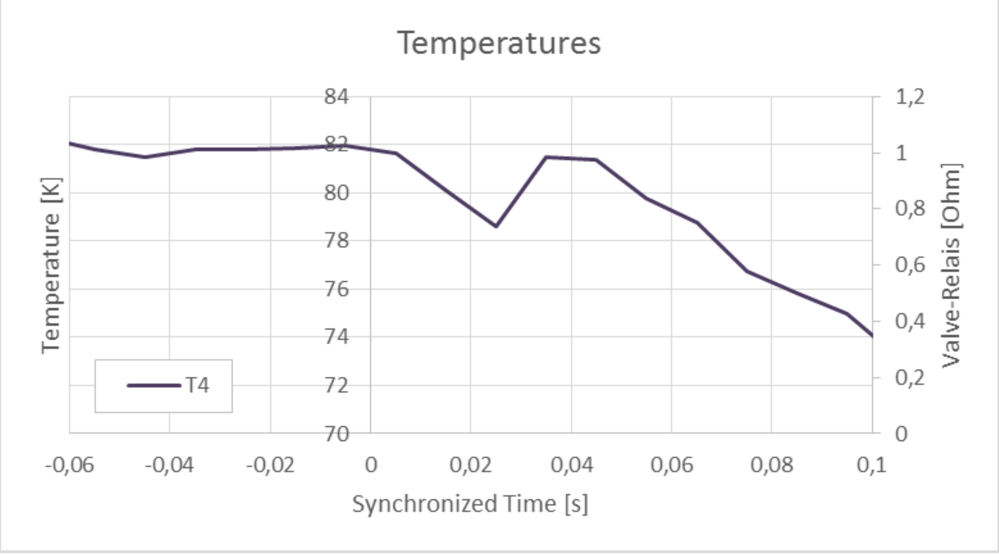

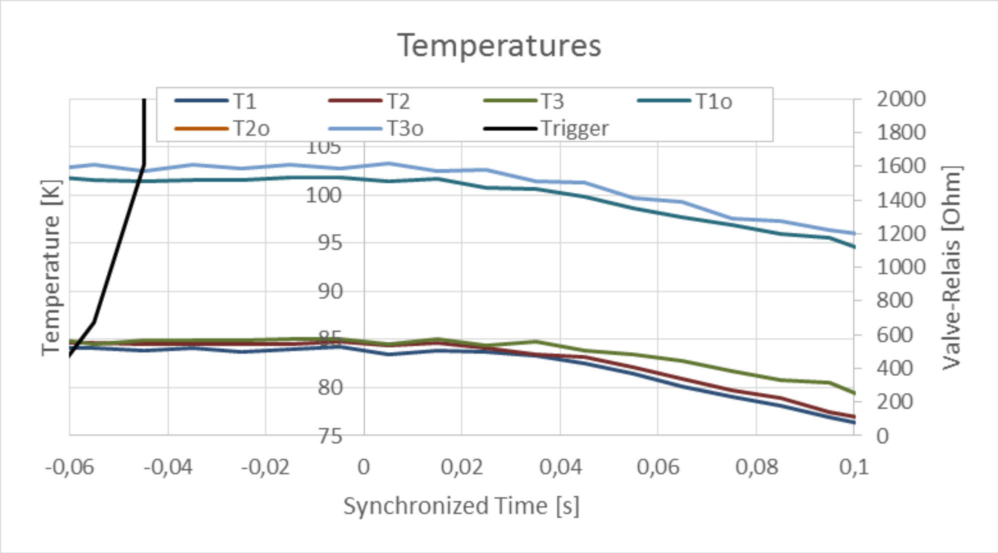
Temperatures
T1
T2
T3
T1o
T2o
T3o
Trigger
Temperature [K]
Valve-Relais [Ohm]
Synchronized Time [s]

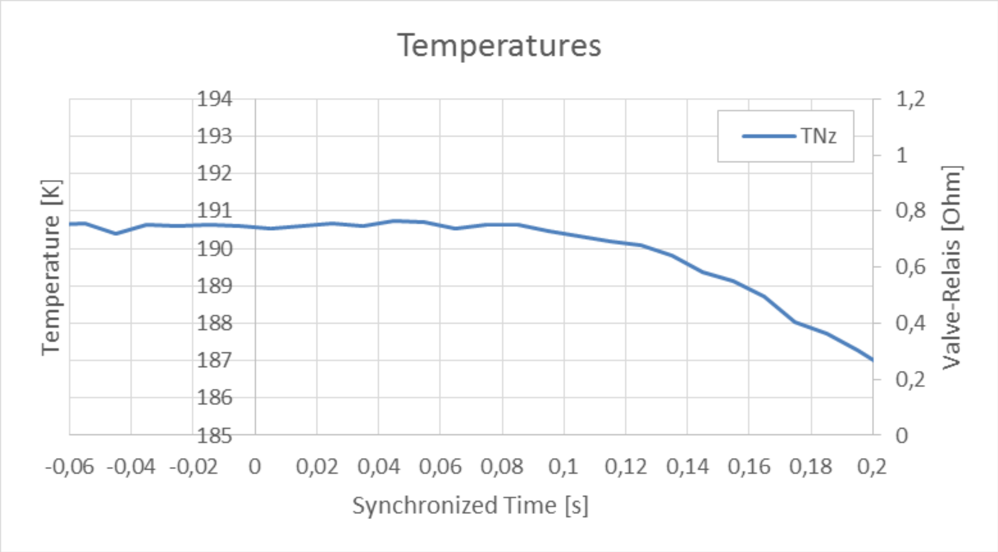
Temperatures
TNz
Temperature [K]
Valve-Relais [Ohm]
Synchronized Time [s]

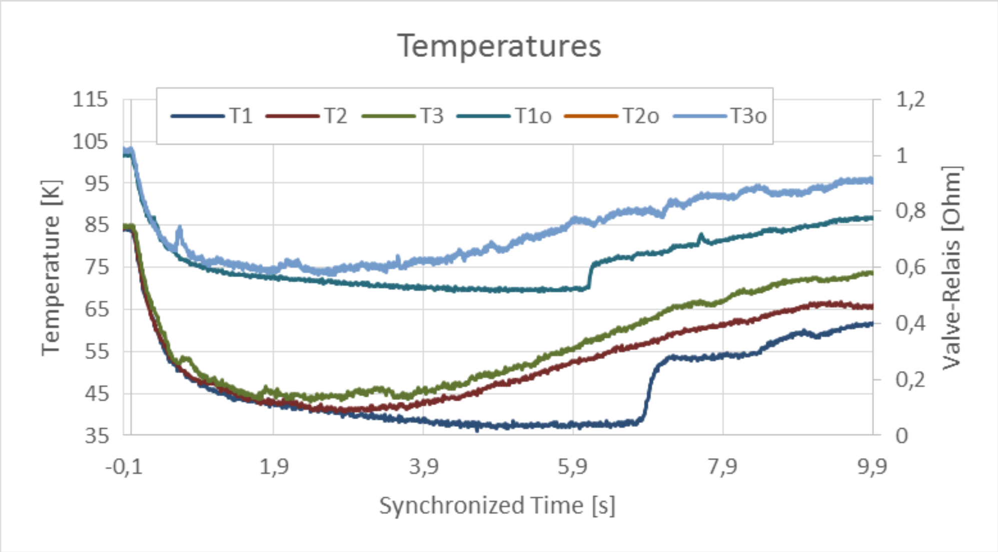
Temperatures
T1
T2
T3
T1o
T2o
T3o
Temperature [K]
Valve-Relais [Ohm]
Synchronized Time [s]

# Appendix A2: All DisCha-Experiments in Sequential Order

## Table 1: Tests of the 1st DisCha campaign at ambient temperature

| Date | Time | dNozz [mm] | pini [bar] | Tini [K] |
|---|---|---|---|---|
| 18.02.2019 | 13:52:40 | 4 | 5 | 290 |
| 18.02.2019 | 13:58:48 | 4 | 5 | 290 |
| 18.02.2019 | 14:02:23 | 4 | 10 | 290 |
| 18.02.2019 | 14:05:30 | 4 | 10 | 290 |
| 18.02.2019 | 14:08:58 | 4 | 20 | 290 |
| 18.02.2019 | 14:13:05 | 4 | 20 | 290 |
| 18.02.2019 | 14:18:49 | 3 | 5 | 290 |
| 18.02.2019 | 14:21:08 | 3 | 5 | 290 |
| 18.02.2019 | 14:23:18 | 3 | 10 | 290 |
| 18.02.2019 | 14:26:24 | 3 | 10 | 290 |
| 18.02.2019 | 14:29:25 | 3 | 20 | 290 |
| 18.02.2019 | 14:33:36 | 3 | 20 | 290 |
| 18.02.2019 | 14:39:22 | 2 | 5 | 290 |
| 18.02.2019 | 14:41:47 | 2 | 5 | 290 |
| 18.02.2019 | 14:43:58 | 2 | 10 | 290 |
| 18.02.2019 | 14:47:13 | 2 | 10 | 290 |
| 18.02.2019 | 14:50:02 | 2 | 20 | 290 |
| 18.02.2019 | 14:54:11 | 2 | 20 | 290 |
| 18.02.2019 | 14:59:37 | 1 | 5 | 290 |
| 18.02.2019 | 15:02:03 | 1 | 5 | 290 |
| 18.02.2019 | 15:05:28 | 1 | 10 | 290 |
| 18.02.2019 | 15:08:51 | 1 | 10 | 290 |
| 18.02.2019 | 11:11:40 | 1 | 20 | 290 |
| 18.02.2019 | 15:16:21 | 1 | 20 | 290 |
| 18.02.2019 | 15:28:03 | 0,5 | 5 | 290 |
| 18.02.2019 | 15:32:11 | 0,5 | 5 | 290 |
| 18.02.2019 | 15:35:16 | 0,5 | 10 | 290 |
| 18.02.2019 | 15:40:48 | 0,5 | 10 | 290 |
| 18.02.2019 | 15:43:18 | 0,5 | 20 | 290 |
| 18.02.2019 | 15:45:10 | 0,5 | 20 | 290 |
| 21.02.2019 | 10:53:23 | 4 | 5 | 290 |
| 21.02.2019 | 11:02:29 | 4 | 10 | 290 |
| 21.02.2019 | 11:05:11 | 4 | 50 | 290 |
| 21.02.2019 | 11:12:57 | 4 | 50 | 290 |
| 21.02.2019 | 14:03:24 | 4 | 100 | 290 |
| 21.02.2019 | 14:05:17 | 4 | 100 | 290 |
| 21.02.2019 | 14:18:46 | 4 | 100 | 290 |
| 21.02.2019 | 14:24:31 | 4 | 150 | 290 |

| | | | | |
|---|---|---|---|---|
| 21.02.2019 | 14:28:19 | 4 | 150 | 290 |
| 21.02.2019 | 14:31:29 | 4 | 200 | 290 |
| 21.02.2019 | 14:34:24 | 4 | 200 | 290 |
| 21.02.2019 | 14:39:34 | 2 | 200 | 290 |
| 21.02.2019 | 14:48:01 | 2 | 200 | 290 |
| 21.02.2019 | 14:56:09 | 2 | 200 | 290 |
| 21.02.2019 | 15:01:10 | 2 | 200 | 290 |
| 21.02.2019 | 15:06:08 | 2 | 150 | 290 |
| 21.02.2019 | 15:09:50 | 2 | 150 | 290 |
| 07.03.2019 | 11:18:16 | 2 | 51,51 | 290 |
| 07.03.2019 | 11:35:13 | 2 | 52,158 | 290 |
| 07.03.2019 | 11:38:15 | 2 | 100 | 290 |
| 07.03.2019 | 11:41:05 | 2 | 150 | 290 |
| 07.03.2019 | 11:49:18 | 2 | 200 | 290 |
| 07.03.2019 | 13:31:59 | 4 | 53,8 | 290 |
| 07.03.2019 | 13:34:54 | 4 | 100 | 290 |
| 07.03.2019 | 13:43:40 | 4 | 200 | 290 |
| 07.03.2019 | 13:53:27 | 4 | 151 | 290 |
| 07.03.2019 | 14:03:03 | 4 | 200 | 290 |
| 07.03.2019 | 14:10:26 | 1 | 54 | 290 |
| 07.03.2019 | 14:13:24 | 1 | 104 | 290 |
| 07.03.2019 | 14:16:56 | 1 | 200 | 290 |
| 07.03.2019 | 14:24:36 | 1 | 150 | 290 |
| 07.03.2019 | 14:37:03 | 0,5 | 53,85 | 290 |
| 07.03.2019 | 14:41:22 | 0,5 | 100 | 290 |
| 07.03.2019 | 14:44:58 | 0,5 | 150 | 290 |
| 07.03.2019 | 14:49:04 | 0,5 | 200 | 290 |
| 12.03.2019 | 14:07:42 | 0,5 | 5 | 290 |
| 12.03.2019 | 14:10:24 | 0,5 | 10 | 290 |
| 12.03.2019 | 14:16:36 | 1 | 5 | 290 |
| 12.03.2019 | 14:19:09 | 1 | 10 | 290 |
| 12.03.2019 | 14:24:44 | 2 | 5 | 290 |
| 12.03.2019 | 14:27:06 | 2 | 10 | 290 |
| 12.03.2019 | 14:32:16 | 4 | 5 | 290 |
| 12.03.2019 | 14:38:46 | 4 | 10 | 290 |

### Table 2: Tests of the 2nd DisCha campaign at ambient temperature

| Date | Time | dNozz [mm] | pini [bar] | Tini [K] |
|---|---|---|---|---|
| 22.03.2019 | 10:06:45 | 4 | 200 | 290 |
| 22.03.2019 | 10:30:08 | 4 | 150 | 290 |
| 22.03.2019 | 10:47:48 | 4 | 100 | 290 |
| 26.03.2019 | 13:47:58 | 2 | 200 | 290 |
| 26.03.2019 | 13:53:13 | 2 | 150 | 290 |
| 26.03.2019 | 13:57:07 | 2 | 100 | 290 |
| 26.03.2019 | 14:00:34 | 2 | 100 | 290 |
| 26.03.2019 | 14:04:41 | 2 | 50 | 290 |
| 26.03.2019 | 14:07:52 | 2 | 50 | 290 |
| 26.03.2019 | 14:19:16 | 1 | 200 | 290 |
| 26.03.2019 | 14:25:23 | 1 | 200 | 290 |
| 26.03.2019 | 14:29:58 | 1 | 150 | 290 |
| 26.03.2019 | 14:34:12 | 1 | 150 | 290 |
| 26.03.2019 | 14:37:50 | 1 | 100 | 290 |
| 26.03.2019 | 14:41:09 | 1 | 100 | 290 |
| 26.03.2019 | 14:45:06 | 1 | 50 | 290 |
| 26.03.2019 | 14:47:55 | 1 | 50 | 290 |
| 26.03.2019 | 14:54:58 | 0,5 | 200 | 290 |
| 26.03.2019 | 15:00:07 | 0,5 | 200 | 290 |
| 26.03.2019 | 15:04:40 | 0,5 | 150 | 290 |
| 26.03.2019 | 15:08:54 | 0,5 | 150 | 290 |
| 26.03.2019 | 15:14:58 | 0,5 | 100 | 290 |
| 26.03.2019 | 15:19:31 | 0,5 | 100 | 290 |
| 26.03.2019 | 15:23:15 | 0,5 | 50 | 290 |

### Table 3: Tests of the 1st DisCha campaign at $LN_2$-temperature

| Date | Time | dNozz [mm] | pini [bar] | Tini [K] |
|---|---|---|---|---|
| 23.04.2019 | 11:19:03 | 2 | 38,3 | 85 |
| 23.04.2019 | 11:29:01 | 2 | 75 | 87 |
| 23.04.2019 | 11:39:51 | 2 | 75 | 87 |
| 23.04.2019 | 11:49:28 | 2 | 76,2 | 86 |
| 23.04.2019 | 12:03:05 | 2 | 110 | 87 |
| 23.04.2019 | 12:14:41 | 2 | 148 | 86 |
| 30.04.2019 | 10:24:56 | 2 | 200 | 82 |
| 30.04.2019 | 11:06:43 | 2 | 200 | 82 |
| 30.04.2019 | 11:18:36 | 2 | 100,8 | 84 |
| 30.04.2019 | 11:40:28 | 2 | 108 | 84 |
| 30.04.2019 | 13:51:53 | 2 | 150 | 84 |
| 30.04.2019 | 14:07:32 | 2 | 150 | 85 |
| 30.04.2019 | 14:14:45 | 2 | 51,9 | 84 |
| 30.04.2019 | 14:25:46 | 2 | 52 | 84 |
| 30.04.2019 | 14:31:05 | 2 | 22,8 | 84 |
| 30.04.2019 | 14:43:08 | 2 | 22,9 | 84 |
| 30.04.2019 | 14:49:09 | 2 | 12,4 | 84 |
| 30.04.2019 | 15:06:00 | 2 | 11,5 | 84 |
| 30.04.2019 | 15:08:17 | 2 | 6 | 84 |
| 30.04.2019 | 15:11:17 | 2 | 5,2 | 84 |
| 03.05.2019 | 10:01:44 | 4 | 151,9 | 84 |
| 03.05.2019 | 10:26:00 | 4 | 150,9 | 84 |
| 03.05.2019 | 10:41:21 | 4 | 101,8 | 84 |
| 03.05.2019 | 10:52:50 | 4 | 101,6 | 84 |
| 03.05.2019 | 11:02:59 | 4 | 22,2 | 84 |
| 03.05.2019 | 11:09:55 | 4 | 11,9 | 84 |
| 03.05.2019 | 11:15:25 | 4 | 10,4 | 84 |
| 03.05.2019 | 11:20:24 | 4 | 5,3 | 84 |
| 03.05.2019 | 11:24:08 | 4 | 5,05 | 85 |
| 03.05.2019 | 11:53:34 | 4 | 50,8 | 84 |
| 03.05.2019 | 12:07:19 | 4 | 48,9 | 84 |
| 03.05.2019 | 12:16:35 | 4 | 20,4 | 84 |
| 03.05.2019 | 13:45:36 | 4 | 201,2 | 84 |
| 03.05.2019 | 14:00:45 | 4 | 200,4 | 84 |
| 07.05.2019 | 13:56:05 | 1 | 153 | 84 |
| 07.05.2019 | 14:14:57 | 1 | 153 | 84 |
| 07.05.2019 | 14:32:57 | 1 | 103 | 84 |
| 07.05.2019 | 14:46:31 | 1 | 99,9 | 81,9 |
| 07.05.2019 | 15:02:52 | 1 | 52,5 | 84 |
| 07.05.2019 | 15:12:56 | 1 | 50 | 86 |

| | | | | |
|---|---|---|---|---|
| 07.05.2019 | 15:23:21 | 1 | 20,1 | 85 |
| 07.05.2019 | 15:30:41 | 1 | 20,1 | 86 |
| 07.05.2019 | 15:37:53 | 1 | 10,1 | 86 |
| 07.05.2019 | 15:46:09 | 1 | 10,4 | 86 |
| 07.05.2019 | 15:53:08 | 1 | 5 | 85 |
| 07.05.2019 | 16:00:47 | 1 | 5,2 | 85 |
| 09.05.2019 | 10:09:55 | 0,5 | 200 | 85 |
| 09.05.2019 | 10:25:57 | 0,5 | 201 | 85 |
| 09.05.2019 | 10:41:38 | 0,5 | 150,5 | 85 |
| 09.05.2019 | 10:53:44 | 0,5 | 150 | 85 |
| 09.05.2019 | 13:27:31 | 0,5 | 100 | 84 |
| 09.05.2019 | 13:45:35 | 0,5 | 100 | 86 |
| 09.05.2019 | 13:57:57 | 0,5 | 50,5 | 85 |
| 09.05.2019 | 14:11:51 | 0,5 | 51 | 85 |
| 09.05.2019 | 14:14:08 | 0,5 | 21 | 85 |
| 09.05.2019 | 14:22:01 | 0,5 | 20,9 | 85 |
| 09.05.2019 | 14:22:54 | 0,5 | 10,2 | 85 |
| 09.05.2019 | 14:32:52 | 0,5 | 9,6 | 85 |
| 09.05.2019 | 14:39:59 | 0,5 | 4,9 | 85 |
| 09.05.2019 | 14:49:55 | 0,5 | 4,8 | 86 |

## Table 4: Tests of 2nd DisCha campaign at $LN_2$ temperature

| Date | Time | dNozz [mm] | pini [bar] | Tini [K] |
|---|---|---|---|---|
| 28.05.2019 | 10:42:04 | 4 | 200 | 84 |
| 28.05.2019 | 10:54:37 | 4 | 50 | 84 |
| 28.05.2019 | 11:04:41 | 4 | 23 | 83 |
| 28.05.2019 | 11:12:40 | 4 | 10 | 83 |
| 28.05.2019 | 11:19:18 | 4 | 5 | 83 |
| 28.05.2019 | 11:28:37 | 4 | 98 | 86 |
| 28.05.2019 | 14:20:48 | 4 | 150 | 84 |
| 28.05.2019 | 14:36:08 | 4 | 100 | 83 |
| 31.05.2019 | 09:49:51 | 2 | 201,5 | 85 |
| 31.05.2019 | 10:02:57 | 2 | 150,14 | 85 |
| 31.05.2019 | 10:12:49 | 2 | 100,09 | 85 |
| 31.05.2019 | 10:19:48 | 2 | 50,03 | 85 |
| 31.05.2019 | 10:28:10 | 2 | 19,95 | 85 |
| 31.05.2019 | 10:34:08 | 2 | 9,59 | 85 |
| 31.05.2019 | 10:38:28 | 2 | 4,99 | 85 |
| 31.05.2019 | 11:04:40 | 1 | 200,07 | 86 |
| 31.05.2019 | 11:18:08 | 1 | 150,11 | 86 |
| 31.05.2019 | 11:29:44 | 1 | 100,08 | 86 |
| 31.05.2019 | 11:39:40 | 1 | 49,86 | 86 |
| 31.05.2019 | 11:49:03 | 1 | 19,31 | 86 |
| 31.05.2019 | 11:56:03 | 1 | 10 | 86 |
| 31.05.2019 | 12:03:33 | 1 | 5,09 | 86 |
| 04.06.2019 | 13:45:43 | 0,5 | 200 | 84 |
| 04.06.2019 | 14:06:57 | 0,5 | 150 | 84 |
| 04.06.2019 | 14:27:52 | 0,5 | 100 | 83 |
| 04.06.2019 | 14:44:25 | 0,5 | 50 | 83,7 |
| 04.06.2019 | 14:56:38 | 0,5 | 20 | 84,5 |
| 04.06.2019 | 15:05:15 | 0,5 | 10 | 84 |
| 04.06.2019 | 15:11:50 | 0,5 | 5 | 84 |
| 04.06.2019 | 15:22:54 | 0,5 | 20 | 84 |
| 04.06.2019 | 15:29:05 | 0,5 | 10 | 84 |
| 04.06.2019 | 15:35:21 | 0,5 | 5 | 84 |
| 24.06.2019 | 14:30:40 | 4 | 200 | 300 |
| 24.06.2019 | 14:42:45 | 4 | 150 | 300 |
| 24.06.2019 | 14:50:52 | 4 | 100 | 300 |
| 24.06.2019 | 14:56:15 | 4 | 50 | 300 |
| 24.06.2019 | 15:10:45 | 2 | 200 | 300 |
| 24.06.2019 | 15:17:44 | 2 | 150 | 300 |
| 24.06.2019 | 15:25:00 | 2 | 100 | 300 |